Tokamak Snake MHD Equilibrium States

W. A. Cooper

Ecole Polytechnique Fédérale de Lausanne, Association EURATOM-Confédération Suisse, Centre de Recherches en Physique des Plasmas, CH1015 Lausanne, Switzerland

and

Guest Professor,
National Institute for Fusion Science, Toki City, Japan

ACKNOWLEDGMENTS

- S. P. Hirshman —— ORNL
- EPFL/CRPP: J. P. Graves, O. Sauter, H. Reimerdes, J. Rossel, M. Albergante, D. Pfefferlé, D. Brunetti, F. Halpern, S. Coda, B. P. Duval, A. Pochelon, B. Labit and the TCV-team
- I. T. Chapman —— CCFE
- Torkil Jensen Award Team at GA: O. Schmitz (KFZ Jülich), E. A. Lazarus (ORNL), T. E. Evans, L. Lao, A. D. Turnbull, R. Buttery, J. R. Ferron, M. Fenstermacher, J. R. Ferron, E. Hollman, C. Petty, M. van Zeeland, J. Yu, F. Turco (Columbia), M. J. Lanctot (LLNL), A. J. Cole (Wisconsin), B. Tobias (PPPL)
- NIFS: K. Y. Watanabe, Y. Suzuki, H. Yamada, A. Komori
- JAEA: N. Aiba, M. Yagi, J. Shiraishi, N. Miyato

PRINCIPAL 3D EFFECTS IN TOKAMAKS

- Toroidal Magnetic Field Ripple
  Periodicity $\propto$ Number of toroidal coils

- Test Blanket Modules, Ferritic Inserts, Toroidal Coil Quench
  Periodicity typically $n = 1$

- ELM Control – RMP Coils
  Periodicity typically $n = 3 - 4$

- Spontaneous Internal Helical Structure Formation — typically 'Snakes'
  Periodicity $n = 1$

MOTIVATION

(1) Assume standard tokamak coils (almost axisymmetric boundary)

(2) Solve for internal flux surfaces in equilibrium: $\rho \cancelto{0}{\frac{dV}{dt}} = \underline{J} \times \underline{B} - \underline{\nabla} P$

- Relax axisymmetry constraint in the vacuum and plasma

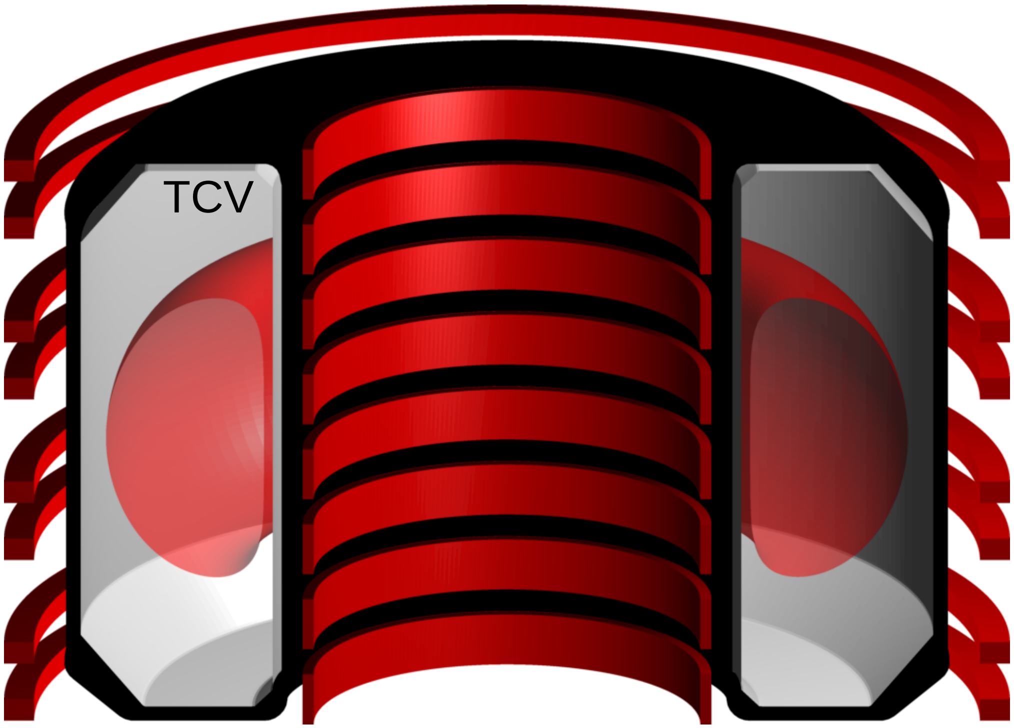

MOTIVATION

(1) Assume standard tokamak coils (almost axisymmetric boundary)

(2) Solve for internal flux surfaces in equilibrium: $\cancel{\rho\frac{dV}{dt}}^{\,0} = \underline{J} \times \underline{B} - \underline{\nabla P}$

- Relax axisymmetry constraint in the vacuum and plasma

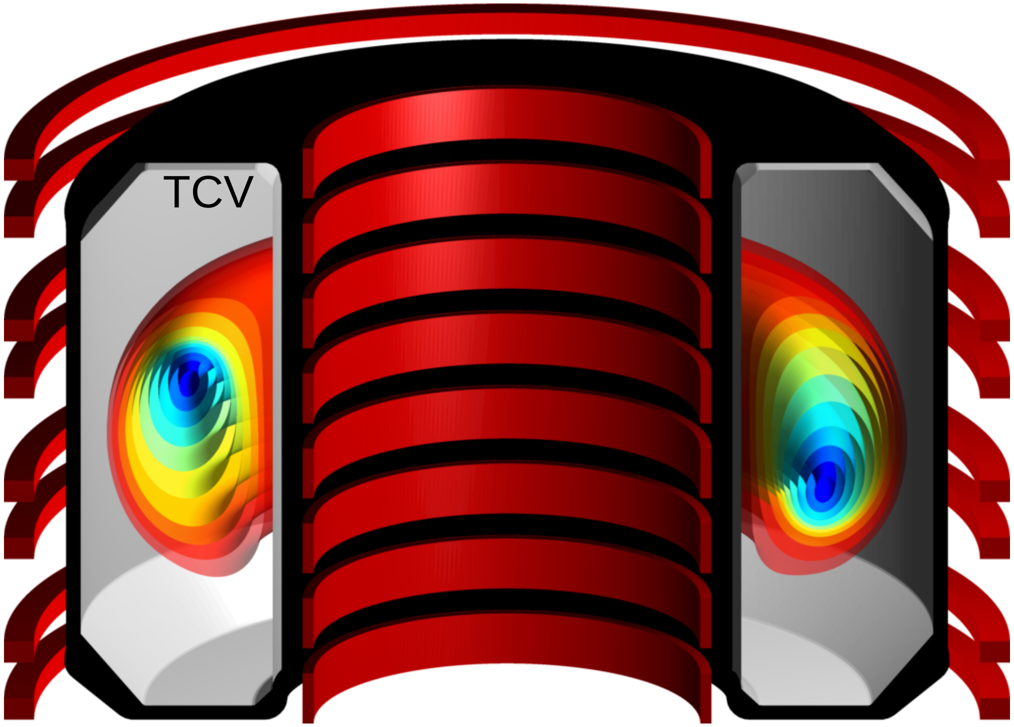

- Two solutions possible. One axisymmetric, the other is helical

- ITER hybrid scenario could be susceptible to helical core deformations

EXPERIMENTAL OBSERVATIONS

Manifestation of internal 3D structures in Tokamaks and RFPs

- SHAx states in RFX-mod

  —R. Lorenzini et al., Nature Physics **5** (2009) 570
- “Snakes” in JET

  —A. Weller et al., Phys. Rev. Lett. **59** (1987) 2303
- Disappearance of sawteeth but continuous dominantly $n = 1$ mode in TCV at high elongation and current —H. Reimerdes et al., PPCF **42** (2006) 629;

  —Y. Camenen et al., Nucl. Fusion **47** (2007) 586
- Long-lived saturated modes in MAST —I. T. Chapman et al., Nucl. Fusion **50** (2010) 045997 and saturated internal kinks in NSTX —J. E. Menard et al., Nucl. Fusion **45** (2005) 539
- Sawteeth vary from kink-like to quasi-interchange-like in DIII-D

  —E. A. Lazarus et al., PPCF **48** (2006) L65

OUTLINE

- We investigate the proposition that the "instability" structures observed in the experiments constitute in reality new equilibrium states with 3D character
- 3D magnetohydrodynamic (MHD) fixed and free boundary equilibria with imposed nested flux surfaces are investigated with the ANIMEC code —W. A. Cooper et al., Comput. Phys. Commun. **180** (2009) 1524
  a version of the VMEC2000 code —S. P. Hirshman, O. Betancourt, J. Comput. Phys. **96** (1991) 99
- Brief review of 3D equilibrium theory
- Fixed boundary snake computations in JET, ITER and DIII-D
- Free boundary TCV equilibrium simulations with 3D helical core structures.
- Conclusions

Magnetohydrodynamic Equilibria — Axisymmetry

- Momentum balance equation

$$\boldsymbol{\nabla} p = \boldsymbol{j} \times \boldsymbol{B}$$

- Parallel projection

$$\boldsymbol{B} \cdot \boldsymbol{\nabla} p = 0 \Longrightarrow p = p(\psi)$$

- Binormal projection

$$\boldsymbol{j} \cdot \boldsymbol{\nabla} \psi = 0 \Longrightarrow I = I(\psi)$$

- Radial projection (Grad-Shafranov equation)

$$\Delta^* \psi = -R^2 p'(\psi) - I(\psi) I'(\psi)$$

- Δ^* operator to solve for $\psi = \psi(R, Z)$ directly

$$\Delta^* = R \frac{\partial}{\partial R} \left(\frac{1}{R} \frac{\partial}{\partial R} \right) + \frac{\partial^2}{\partial Z^2}$$

Magnetohydrodynamic Equilibria — 3D

- Impose nested magnetic surfaces and single magnetic axis
- Minimise energy of the system

$$W = \int\int\int d^3x \Big(\frac{B^2}{2\mu_0} + \frac{p_\parallel(s,B)}{\Gamma - 1} \Big)$$

- Solve inverse equilibrium problem : $R = R(s,u,v)$, $Z = Z(s,u,v)$.

- Variation of the energy

$$\begin{aligned} \frac{dW}{dt} = & - \int\int\int dsdudv \Big[F_R \frac{\partial R}{\partial t} + F_Z \frac{\partial Z}{\partial t} + F_\lambda \frac{\partial \lambda}{\partial t} \Big] \\ & - \int\int_{s=1} dudv \Big[R \Big(p_\perp + \frac{B^2}{2\mu_0} \Big) \Big(\frac{\partial R}{\partial u} \frac{\partial Z}{\partial t} - \frac{\partial Z}{\partial u} \frac{\partial R}{\partial t} \Big) \Big] \end{aligned}$$

Magnetohydrodynamic Equilibria — 3D

- The MHD forces are

$$
\begin{aligned}
F_R = &\quad \frac{\partial}{\partial u}[\sigma\sqrt{g}B^u(\boldsymbol{B}\cdot\boldsymbol{\nabla}R)] + \frac{\partial}{\partial v}[\sigma\sqrt{g}B^v(\boldsymbol{B}\cdot\boldsymbol{\nabla}R)] \\
- &\quad \frac{\partial}{\partial u}\Big[R\frac{\partial Z}{\partial s}\Big(p_\perp + \frac{B^2}{2\mu_0}\Big)\Big] + \frac{\partial}{\partial s}\Big[R\frac{\partial Z}{\partial u}\Big(p_\perp + \frac{B^2}{2\mu_0}\Big)\Big] \\
+ &\quad \frac{\sqrt{g}}{R}\Big[\Big(p_\perp + \frac{B^2}{2\mu_0}\Big) - \sigma R^2 (B^v)^2\Big] \\
F_z = &\quad \frac{\partial}{\partial u}[\sigma\sqrt{g}B^u(\boldsymbol{B}\cdot\boldsymbol{\nabla}Z)] + \frac{\partial}{\partial v}[\sigma\sqrt{g}B^v(\boldsymbol{B}\cdot\boldsymbol{\nabla}Z)] \\
+ &\quad \frac{\partial}{\partial u}\Big[R\frac{\partial R}{\partial s}\Big(p_\perp + \frac{B^2}{2\mu_0}\Big)\Big] - \frac{\partial}{\partial s}\Big[R\frac{\partial R}{\partial u}\Big(p_\perp + \frac{B^2}{2\mu_0}\Big)\Big]
\end{aligned}
$$

- The λ force equation minimises the spectral width and corresponds to the binormal projection of the momentum balance at the equilibrium state.

$$
F_\lambda = \Phi'(s)\Big[\frac{\partial(\sigma B_v)}{\partial u} - \frac{\partial(\sigma B_u)}{\partial v}\Big]
$$

- For isotropic pressure $p_{||} = p_\perp = p$ and $\sigma = 1/\mu_0$.

Magnetohydrodynamic Equilibria — 3D

- Use Fourier decomposition in the periodic angular variables u and v and a special finite difference scheme for the radial discretisation

- An accelerated steepest descent method is applied with matrix preconditioning to obtain the equilibrium state

- The radial force balance is a diagnostic of the accuracy of the equilibrium state in this approach

$$\left\langle \frac{F_s}{\Phi'(s)} \right\rangle = -\left\langle \frac{1}{\Phi'(s)} \frac{\partial p_{\|}}{\partial s}\Big|_B \right\rangle - \frac{\partial}{\partial s}\left\langle \frac{\sigma B_v}{\sqrt{g}} \right\rangle - \iota(s) \frac{\partial}{\partial s}\left\langle \frac{\sigma B_u}{\sqrt{g}} \right\rangle$$

- $\langle \cdots \rangle$ denotes a flux surface average

$$\langle A \rangle = \frac{L}{(2\pi)^2} \int_0^{2\pi/L} dv \int_0^{2\pi} du \sqrt{g} A(s,u,v)$$

- This model is implemented in the ANIMEC code, an anisotropic pressure extension of the VMEC2000 code. L is the number of toroidal field periods.

Fixed Axisymmetric JET Boundary Equilibria

- JET boundary: $R_b = R_0 + a\cos(u + \delta \sin u + \tau \sin 2u)$; $Z_b = Ea \sin u$
  JET: $R_0 = 2.96m$, $a = 1.25m$, $E = 1.68$, $\delta = 0.3$, $\tau = 0$
- Prescribe mass profile and toroidal current profile.
- Equilibrium has toroidal current $3.85MA$, $B_t = 3.1T$, $\langle\beta\rangle \simeq 2.3\%$
- pressure profile

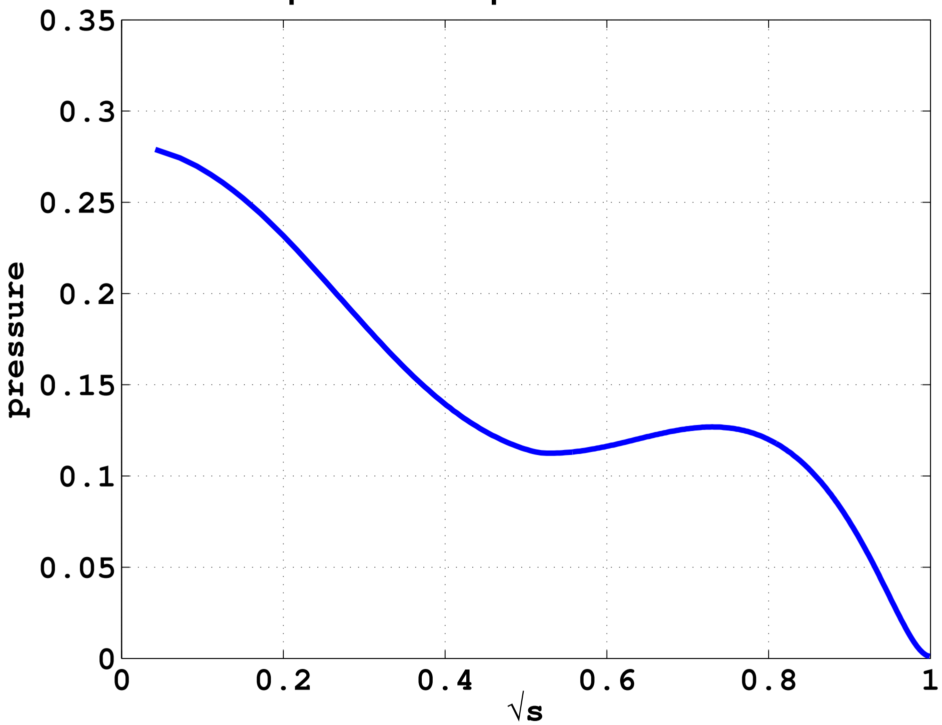

q-profile

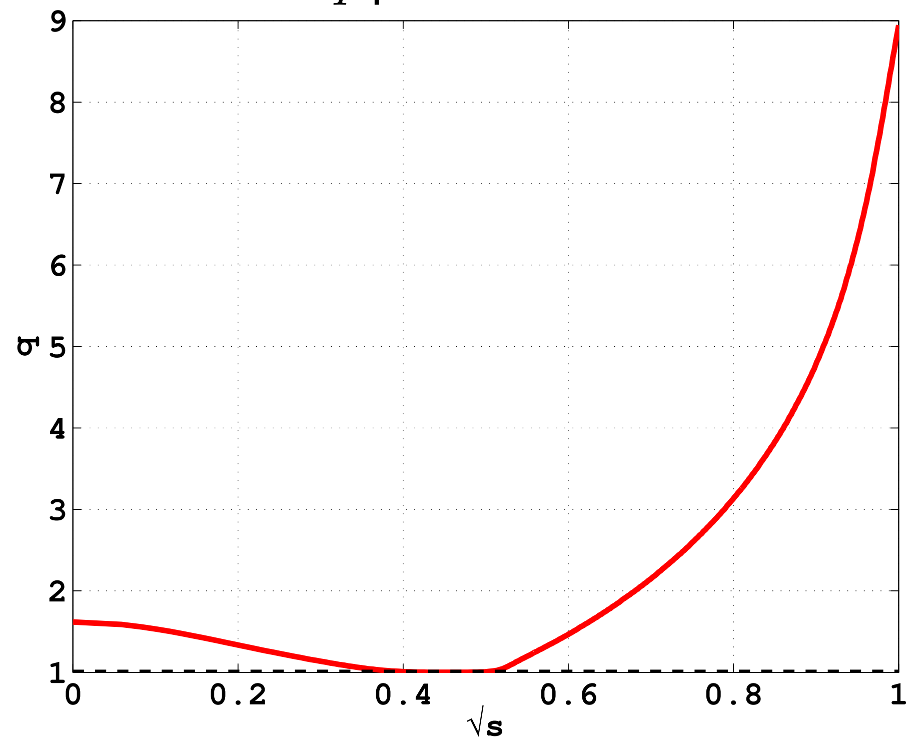

CRPP

"SNAKE" Theory

- JET and many other tokamaks develop long-lived internal helical structures referred to as "snakes" as a result of pellet injection or spontaneously through impurity accumulation *(Weller et al., Phys. Rev. Lett **59** (1987) 2303)*.
- The standard conjecture about the formation of "snakes" was described by *Wesson (Plasma Phys. Control. Fusion **37** (1995) A337-A346)*.

  The magnetic island at the $q = 1$ surface traps some of the ionised pellet material that is maintained by increased resistivity due to impurity accumulation and improved local confinement that increases the density.
- "Snakes' observed on Tore-Supra are localised at a smaller radial position than the $q = 1$ island (*Pecquet et al., Nucl. Fusion **37** (1997) 451.*

"SNAKE" Theory

- We invoke an alternative explanation that applies both to pellet and spontaneously induced snakes.
  The pellet (or the impurities) reach the magnetic axis causing the centre of the plasma to locally cool. The current channel as a result moves radially outward and the hollow current profile leads to reverse magnetic shear with q_{min} *in the neighbourhood of unity. These conditions destabilise an ideal internal kink mode that saturates. The resulting structure constitutes the "snake".*

- We systematically compute "snake" 3D internal helical equilibrium structures with the ANIMEC code in a wide variety of tokamaks (JET, TCV, ITER, MAST, DIII-D)

JET MHD equilibrium solutions bifurcate

- Pressure distribution in a JET axisymmetric and helical “snake” equilibrium

$v = 0$ $v = \pi/3$ $v = 2\pi/3$ $v = \pi$

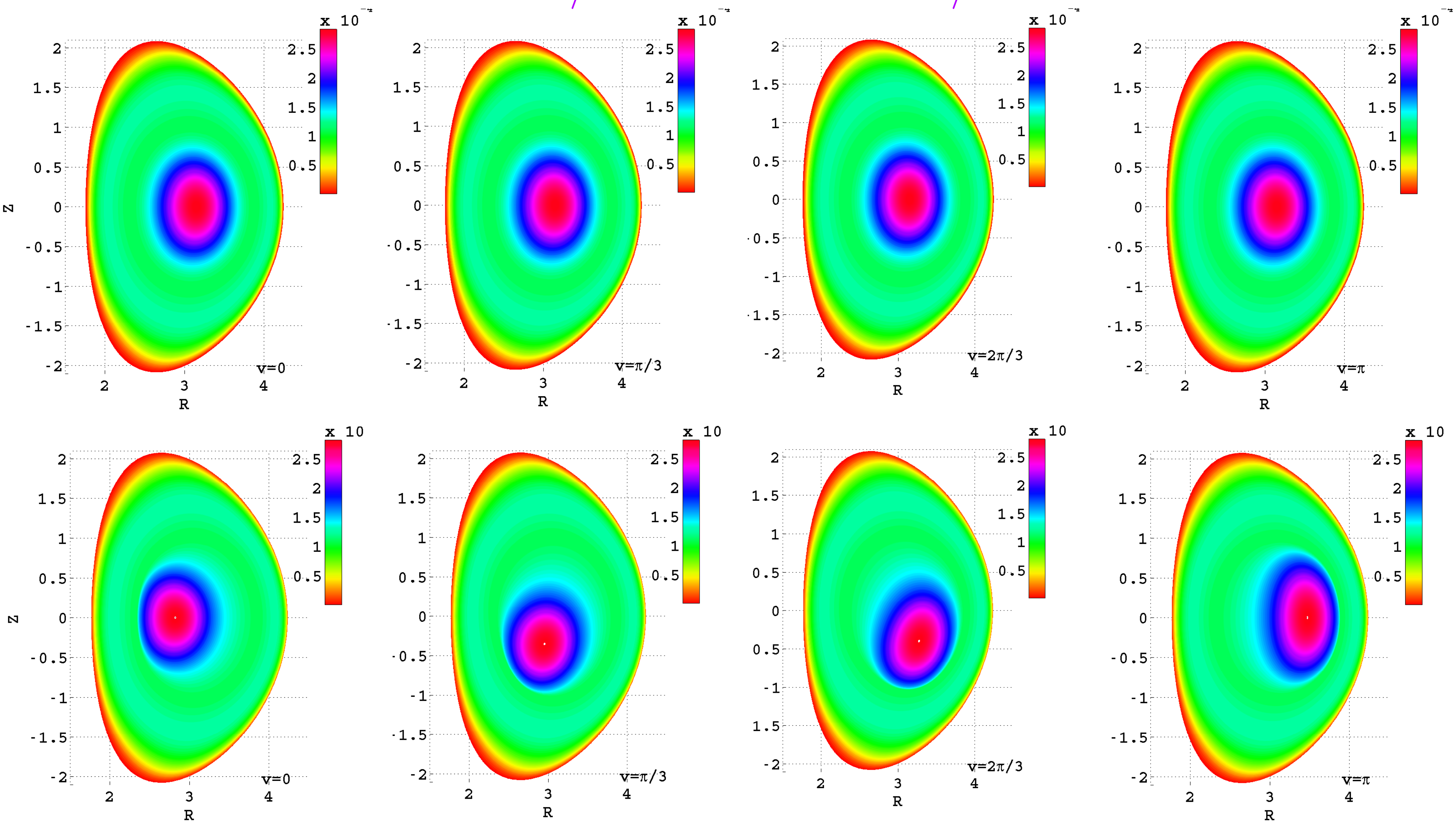

Experiment / simulation comparison

- Standard view of a snake (with variation with respect to toroidal angle in lieu of time in the simulation).

- experiment (courtesy of A. Weller) ANIMEC simulation

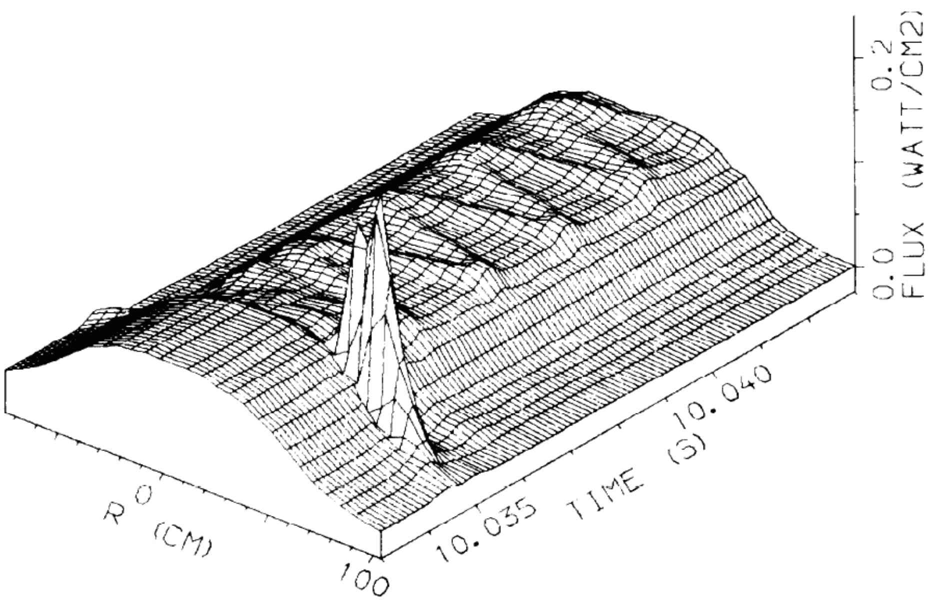

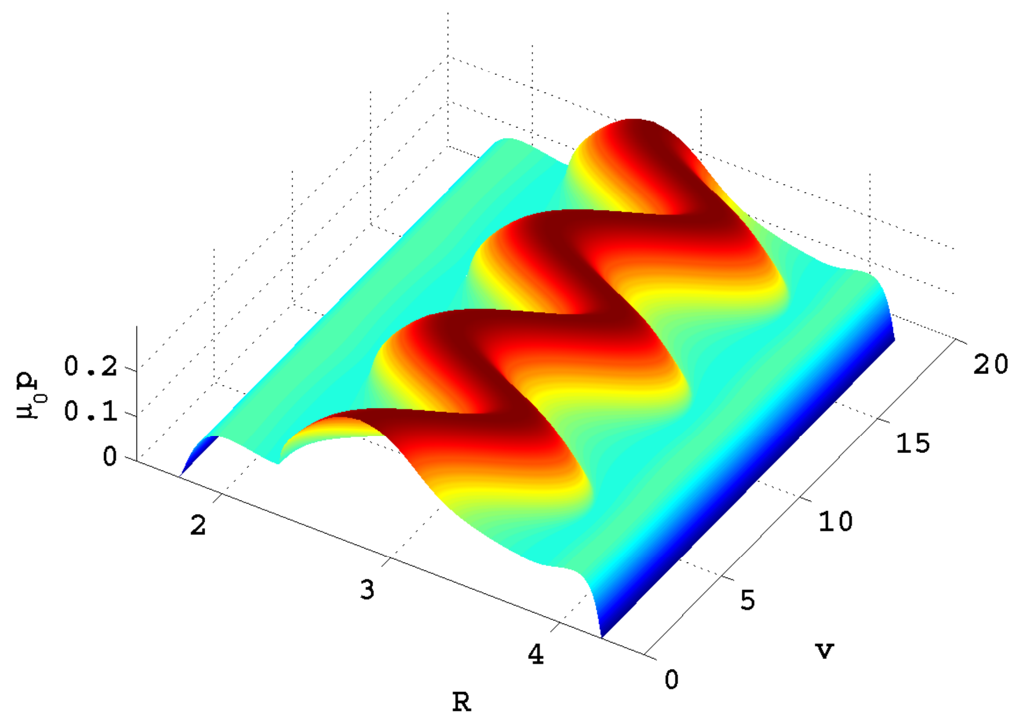

- Static approximation justified: Snake toroidal rotation $\sim 70Hz$, Alfvén wave frequency around the torus $\sim 500kHz$.

JET "snake" structure size

- Variation of the snake size as a function of toroidal current or q_{min}

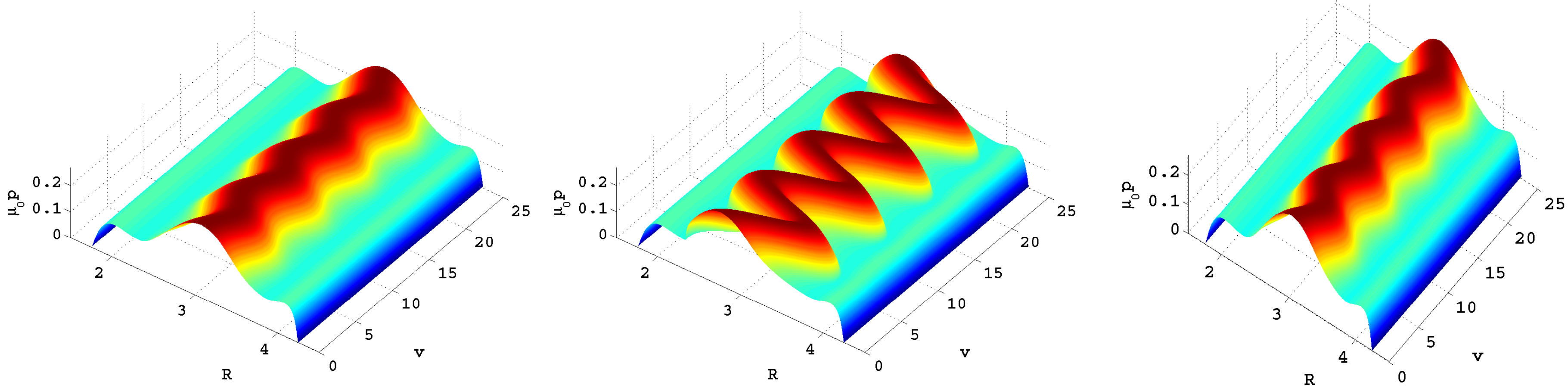

- $I_t = 3.77MA$ $I_t = 3.95MA$ $I_t = 4.07MA$
- $q_{min} \simeq 1.02$ $q_{min} \simeq 1$ $q_{min} \simeq 0.95$

- \- Model predicts 'snake' structures in the range $0.94 < q_{min} < 1.03$ in JET.
  \- $q = 1$ island is not required for 'snake' formation and persistence.
  \- Robust to sawtooth events.

JET "snake" structure at $q_{min} = 0.945$

- Superimposed "snake" structure of the pressure and rotational transform $\iota = 1/q$ when $q_{min} = 0.9452$ $(I_t = 2\pi J_t = 4.07MA)$ demonstrates that the pressure distortions are well inside the $q \leq 1$ domain. This is consistent with the snake observations on Tore Supra.

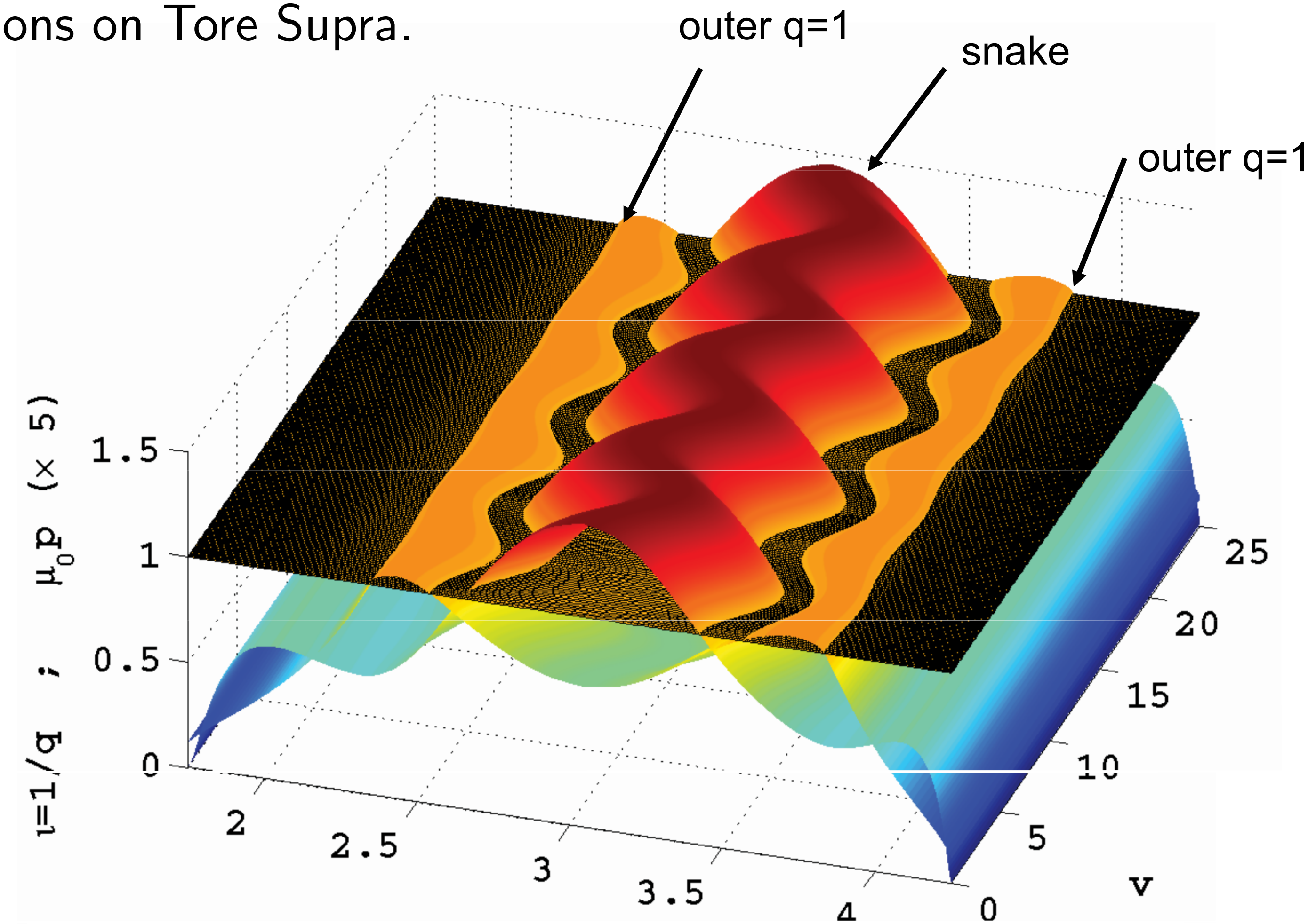

Axis excursion definition

- To quantify dimensions of the helical core, define a magnetic axis helical excursion parameter

$$\delta_H = \frac{\sqrt{R_{01}^2(s=0) + Z_{01}^2(s=0)}}{a}$$

Energy difference and axis distortion

- Compare energy difference between axisymmetric and helical branch solutions
- Axis excursion as a function of q_{min} for helical branch
- Compare with linear ideal kink growth rate of axisymmetric branch
- ΔW of bifurcated branch solutions δ_H and γ

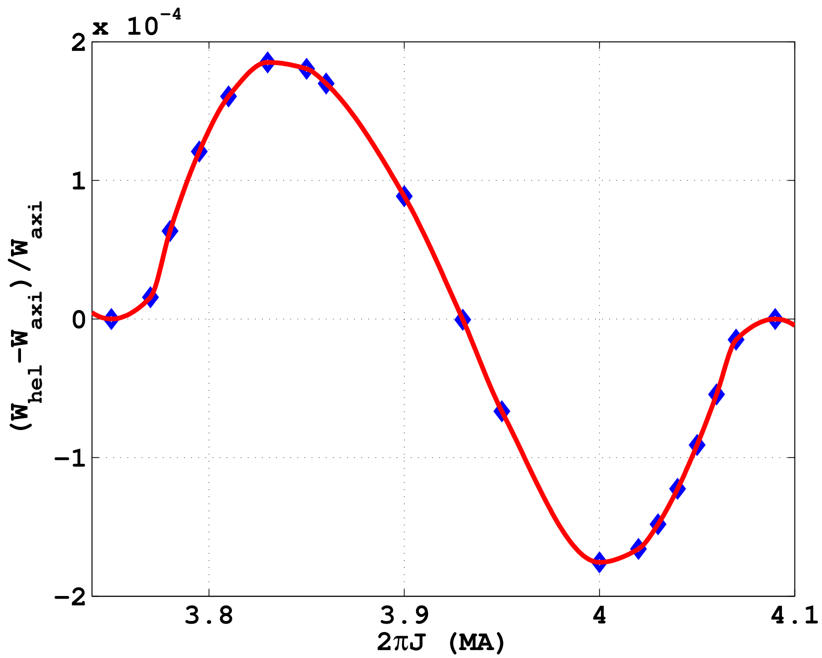

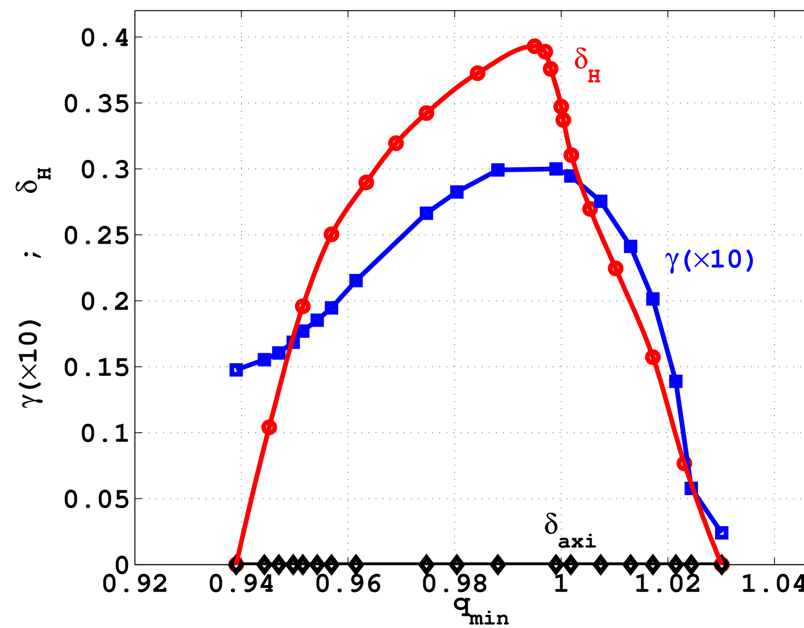

- Energy difference between the two branches is miniscule: $W_{hel} < W_{axi}$ for $q_{min} < 1$, $W_{hel} > W_{axi}$ for $q_{min} > 1$.
- δ_H aligns with γ (growth rate of the kink mode)

JET pressure, mod-B contours at various cross sections

- Contours of constant pressure and mod-B of a JET "snake" equilibrium

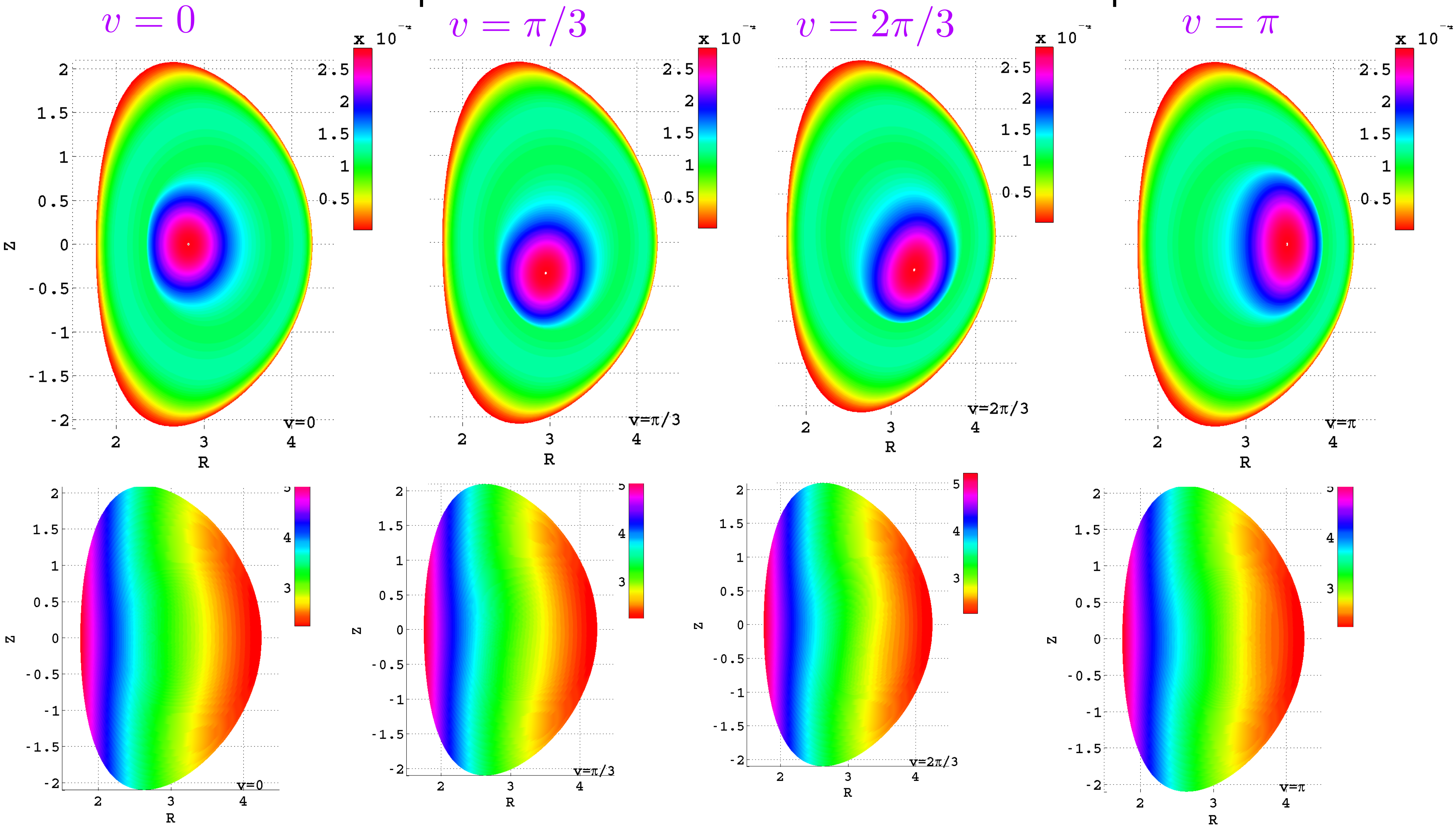

JET “snake” equilibrium convergence

- Convergence to a solution and average radial force balance

- horizontal force   normalised radial force

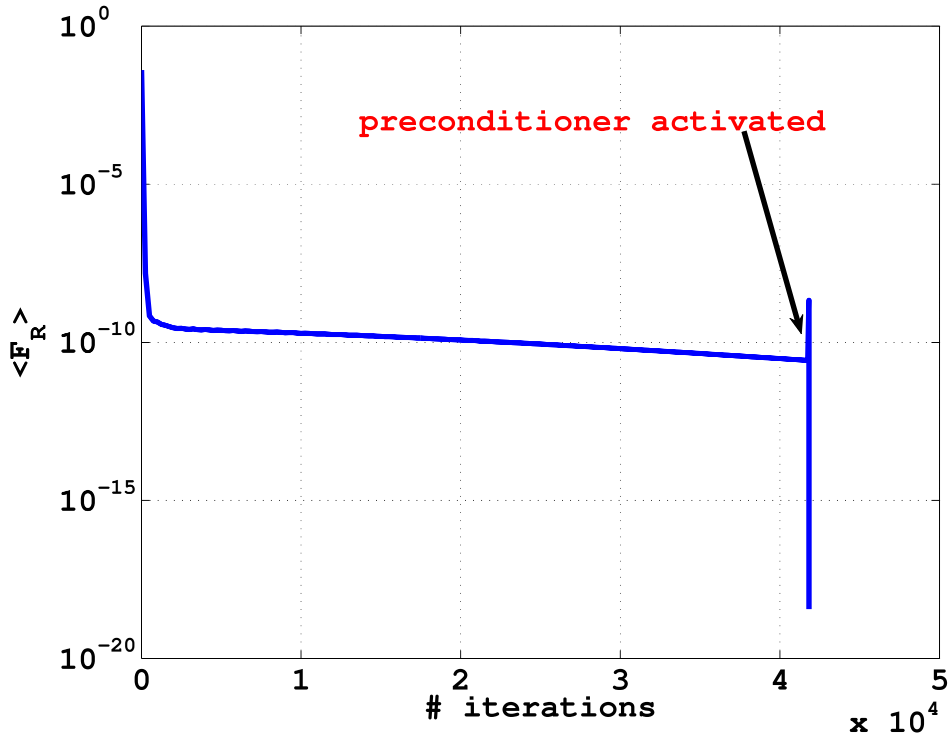

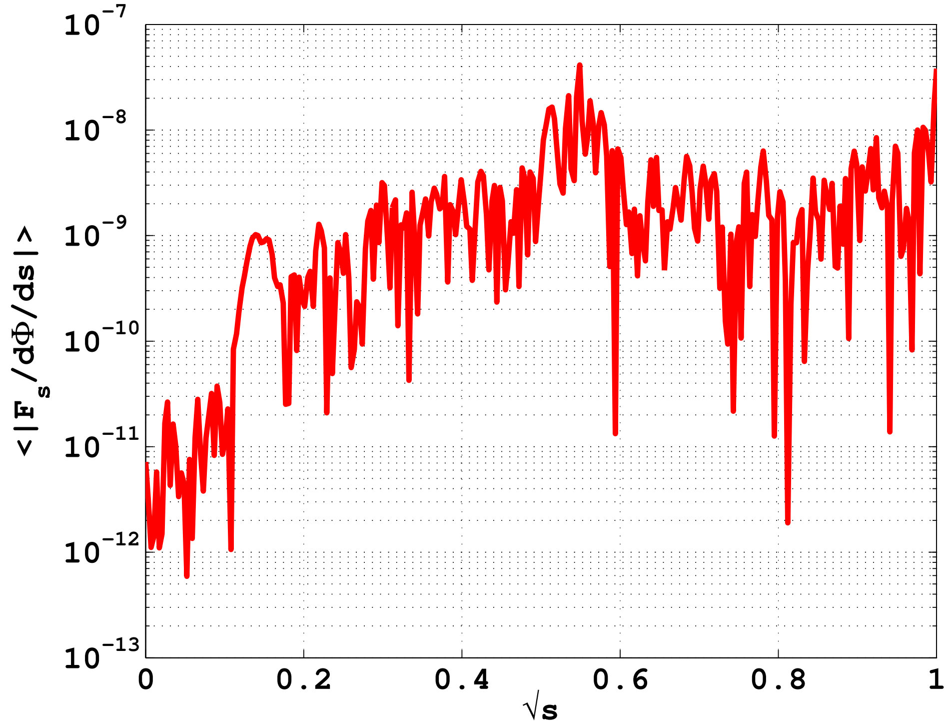

SNAKES IN THE ITER HYBRID SCENARIO

- Contours of constant pressure of an ITER hybrid scenario equilibrium with $13.3MA$ toroidal plasma current

$v = 0$ $\quad$ $v = \pi/3$ $\quad$ $v = 2\pi/3$ $\quad$ $v = \pi$

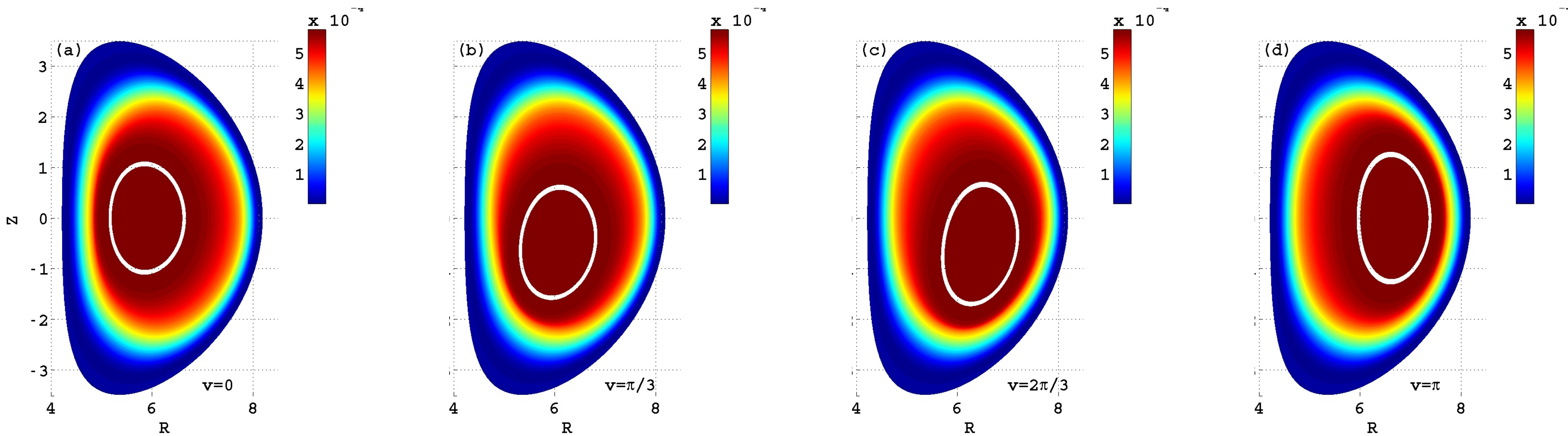

- *"Helical ITER Hybrid Scenario Equilibria",* W. A. Cooper, J. P. Graves and O. Sauter, Plasma. Phys. Control. Fusion **53** (2011) 024002.

ITER equilibrium profiles

- Prescribe mass profile and toroidal current profile. $p(s) \sim \mathcal{M}(s)[\Phi'(s)]^{\Gamma}$
- Equilibria have toroidal current $13 - 14MA$, $B_t = 4.6T$, $\langle\beta\rangle \simeq 2.9\%$
- q-profile | q-profile range for helical states

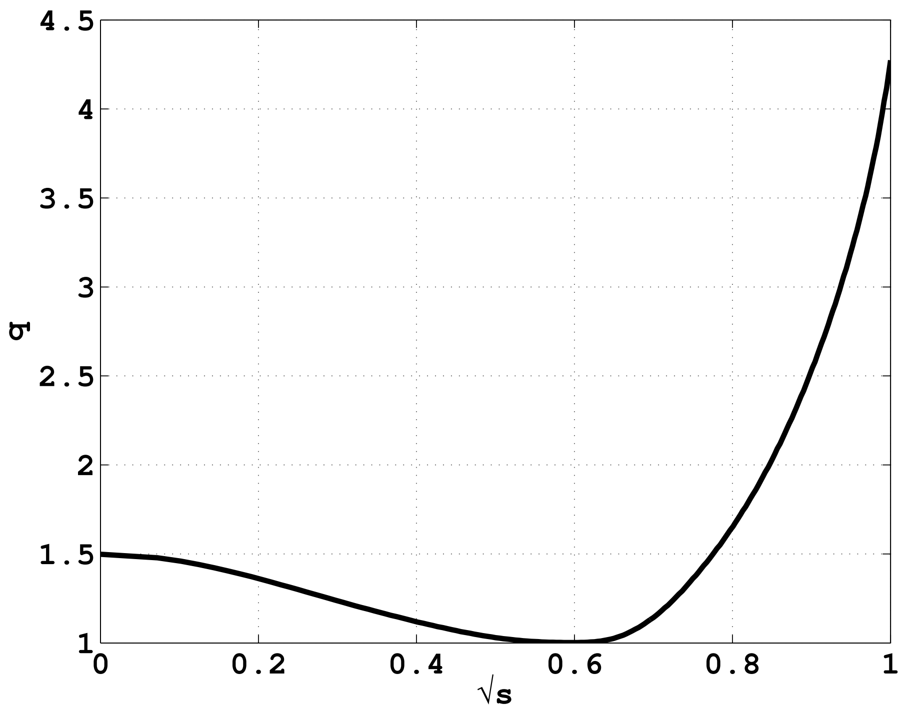

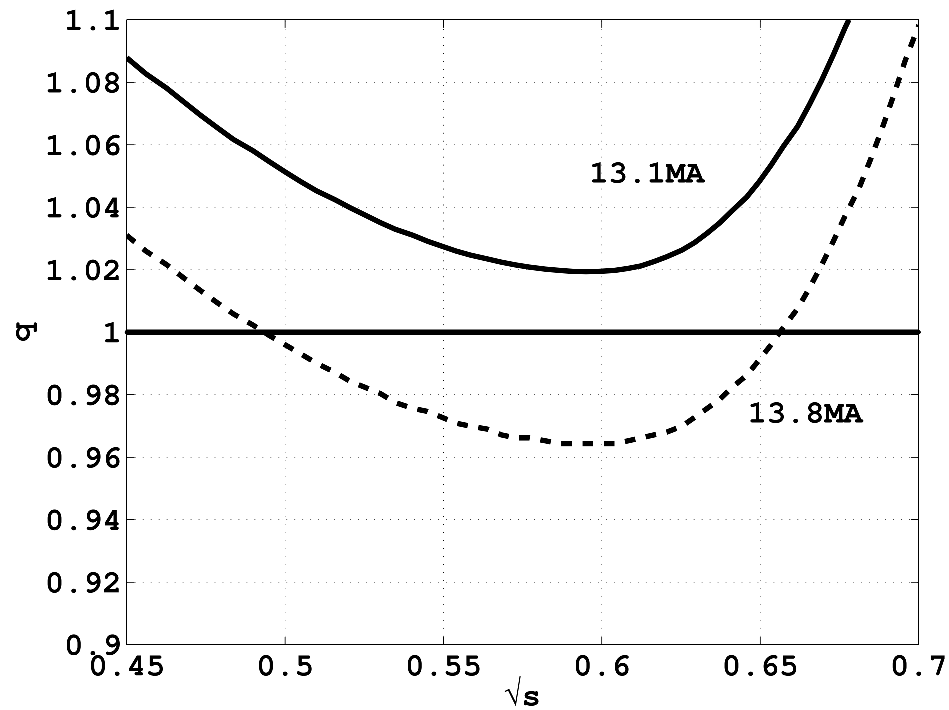

Helical core ITER equilibria

- Variation of the helical axis distortion parameter δ_H with respect to the toroidal current and corresponding variation with respect to q_{min}.

- δ_H versus current δ_H versus q_{min}

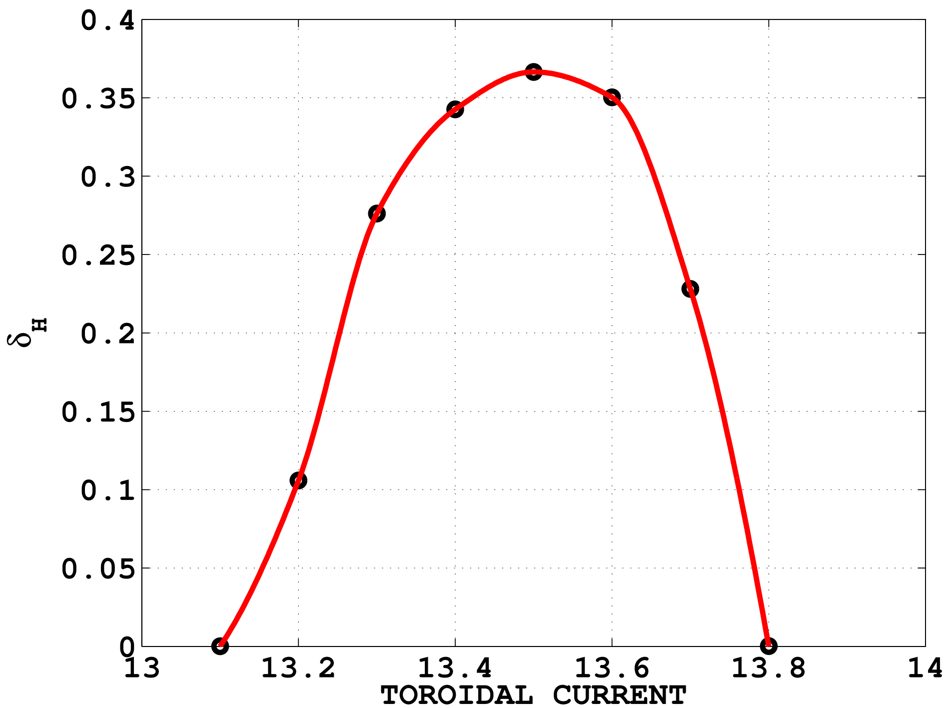

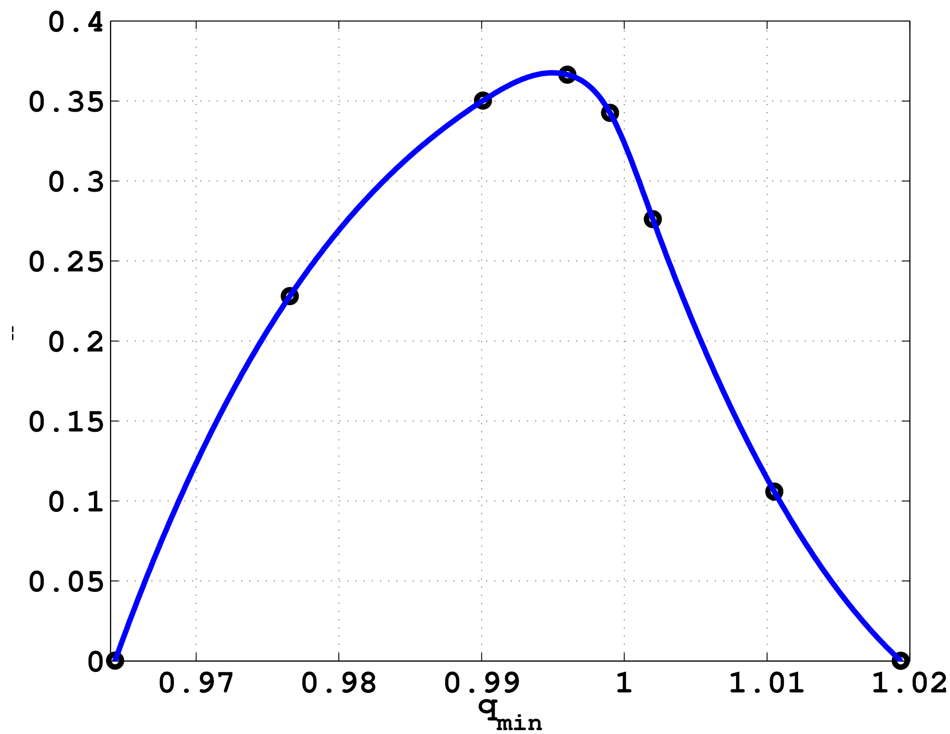

ITER pressure contours as a function of plasma current

- Contours of constant pressure at the cross section with toroidal angle $v = 2\pi/3$

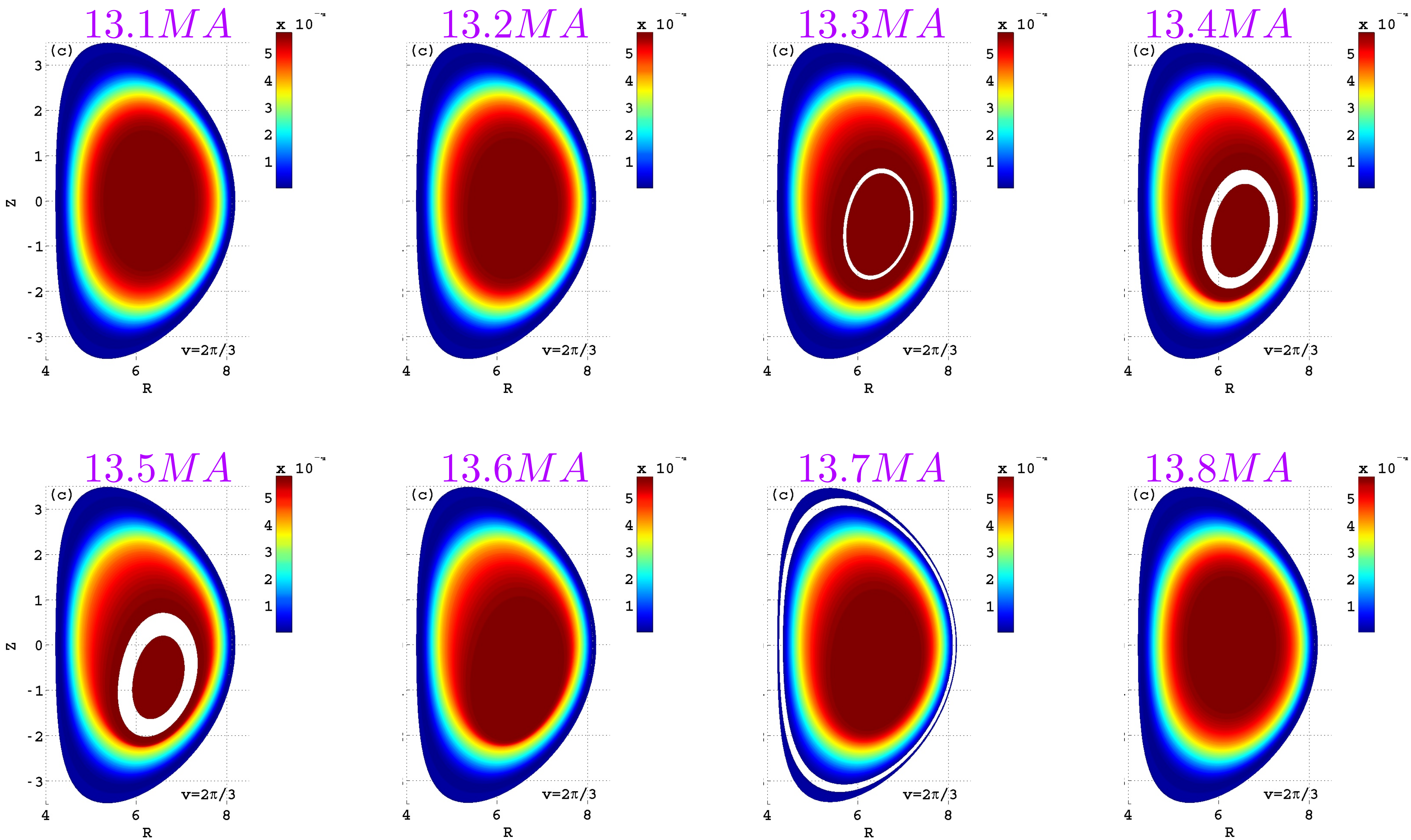

Finite $\langle\beta\rangle$ ITER scan

- The ITER hybrid scenario is projected in the range $12 - 14MA$ with $B_t = 5.3T$. With a sharper core concentrated toroidal current at $12MA$, the variation of the helical axis distortion parameter δ_H with respect to $\langle\beta\rangle$ is computed.

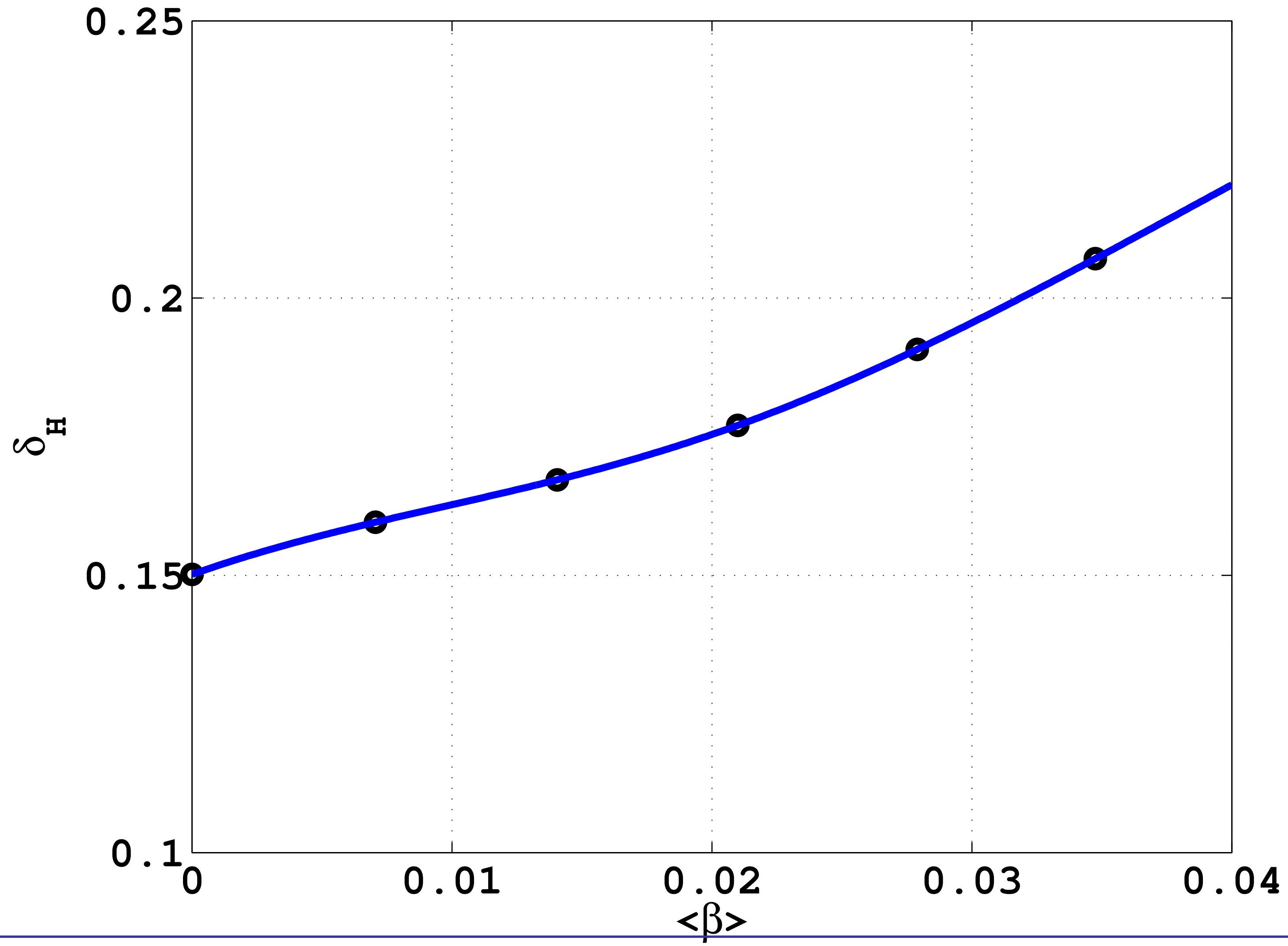

TJA Experiment Simulations for DIII-D

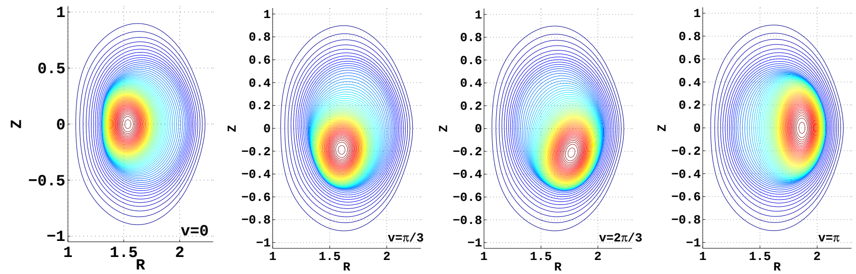

Fig. 1. The normalised plasma pressure distributions in a fixed axi- and up-down symmetric boundary hybrid-scenario oval DIII-D equilibrium calculation at 4 cross sections covering half a field period with toroidal angles $v = 0$, $v = \pi/3$, $v = 2\pi/3$ and $v = \pi$ (from left to right, respectively) at $\langle\beta\rangle \simeq 0.89\%$ and $1.43MA$ toroidal current ($q_b = 4.21$) with prescribed pressure and toroidal current profiles. This equilibrium has $\beta_N \simeq 0.73$ and $\beta_{pol} \simeq 0.24$.

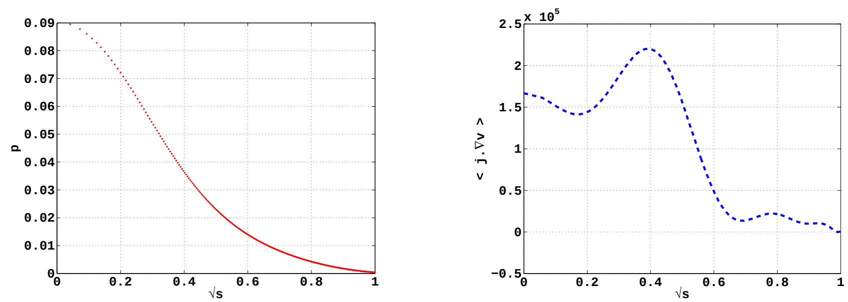

Fig. 2. The input pressure (left) and toroidal current (right) profiles.

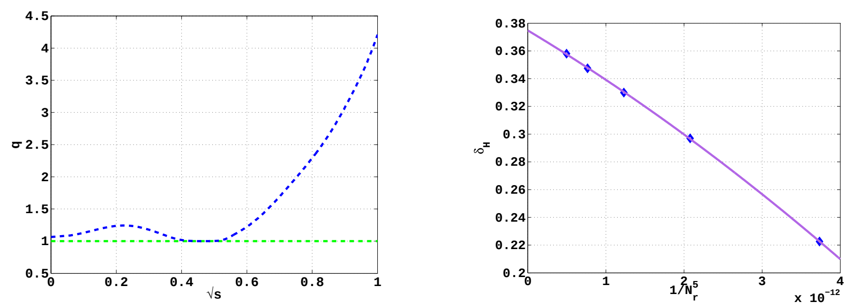

Fig. 3. The resulting q-profile (left) and convergence of the helical excursion of the magnetic axis with respect to the inverse number of radial grid points to the 5th power (right).

Fixed Boundary DIII-D Computations

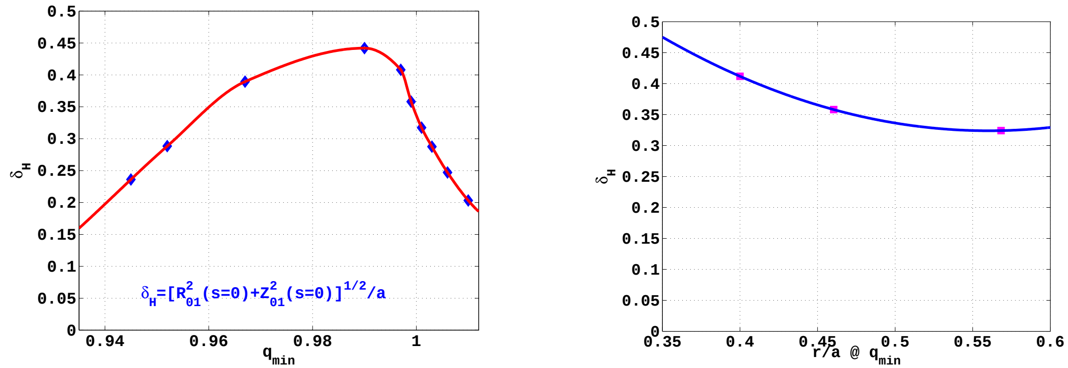

Fig. 1. The helical axis excursion parameter δ_H as a function of q_{min} (left) and as a function of the radial positioning of q_{min} (right) when $q_{min} \simeq 1$. The toroidal current is $2\pi J = 1.43MA$.

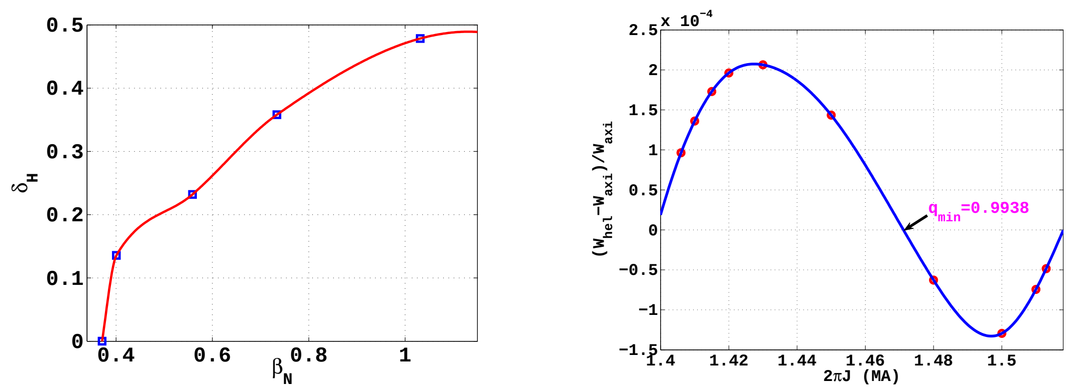

Fig. 2. The helical axis excursion parameter δ_H as a function of β_N with toroidal current $2\pi J \sim 1.43MA$ (left) and the normalised energy difference as a function of the toroidal current (right).

MSE synthetic diagnostic

- A synthetic Motional Stark Effect diagnostic is developed for a DIII-D helical core simulation

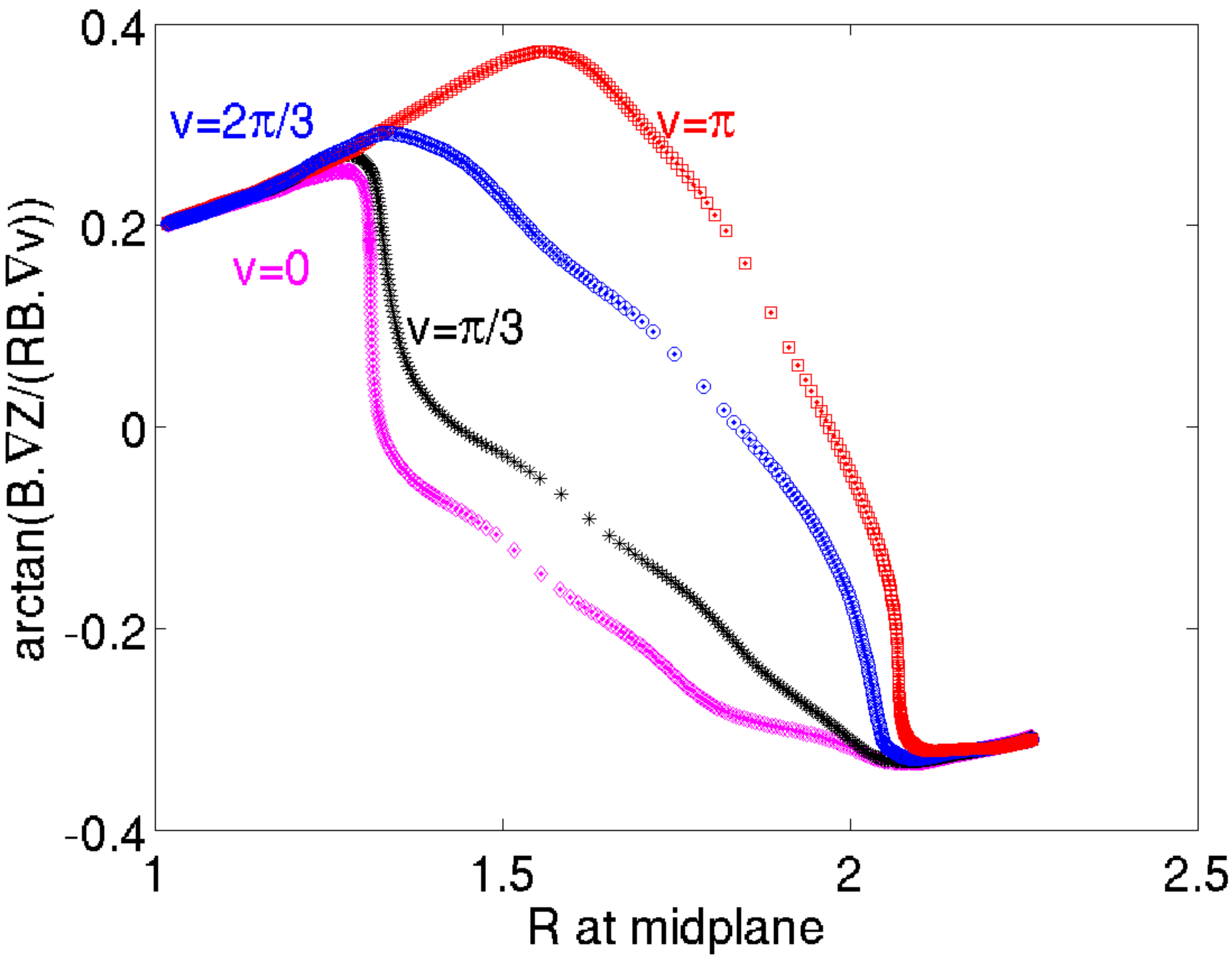

Free Boundary TCV Computations

- TCV coil system shown is modelled with 4 filaments per coil
- The toroidal coils carry $358kA$
- There are 16 poloidal field coils that typically allow up to $238kA$

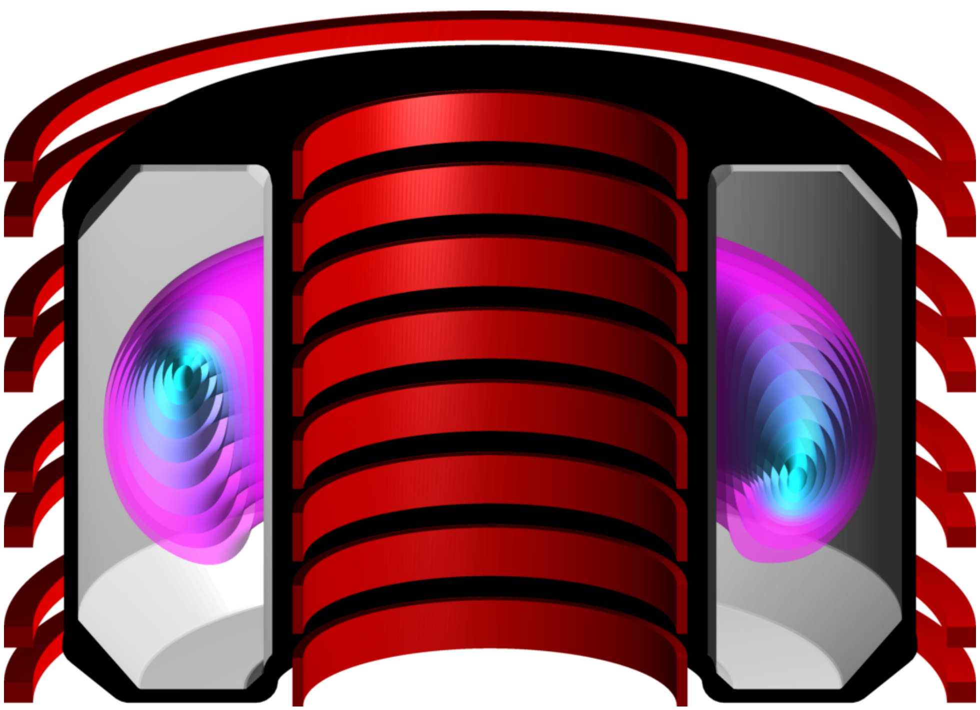

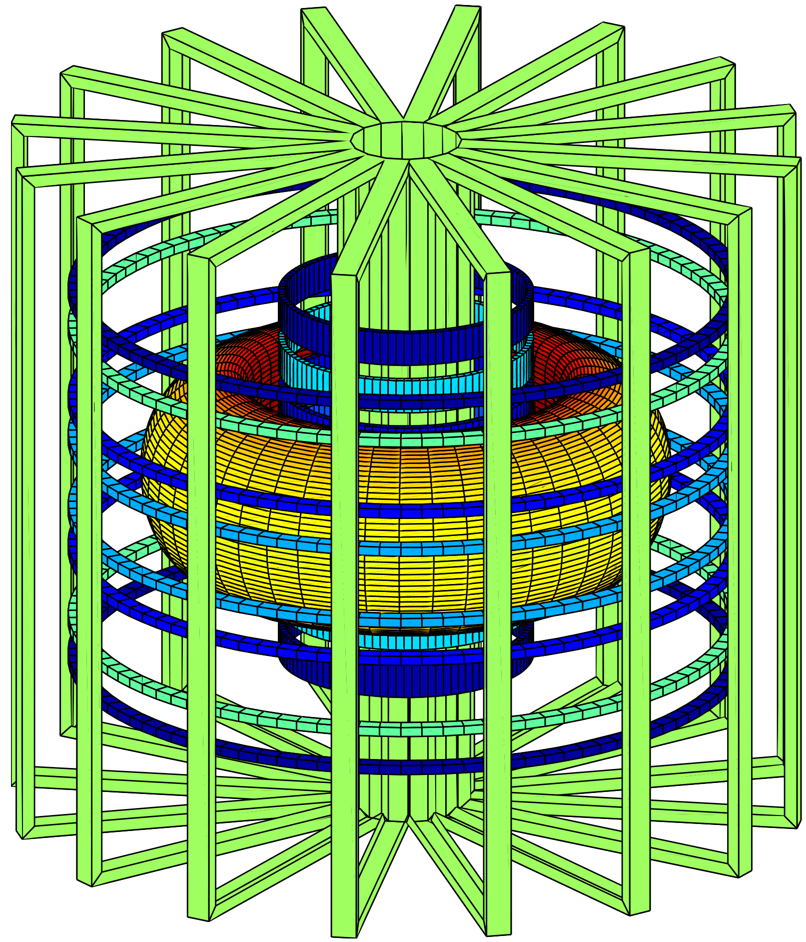

TCV prescribed current and q-profiles at finite $\langle\beta\rangle$

- Toroidal current profile fit to that from a previous run with $1/q$ prescribed, but flattening the edge region

- $2\pi J'(s) = 0.98 + 5.168s - 67.464s^2 + 440.42s^3 - 1391.7s^4 + 2146.5s^5 - 1582.1s^6 + 448.27s^7$.

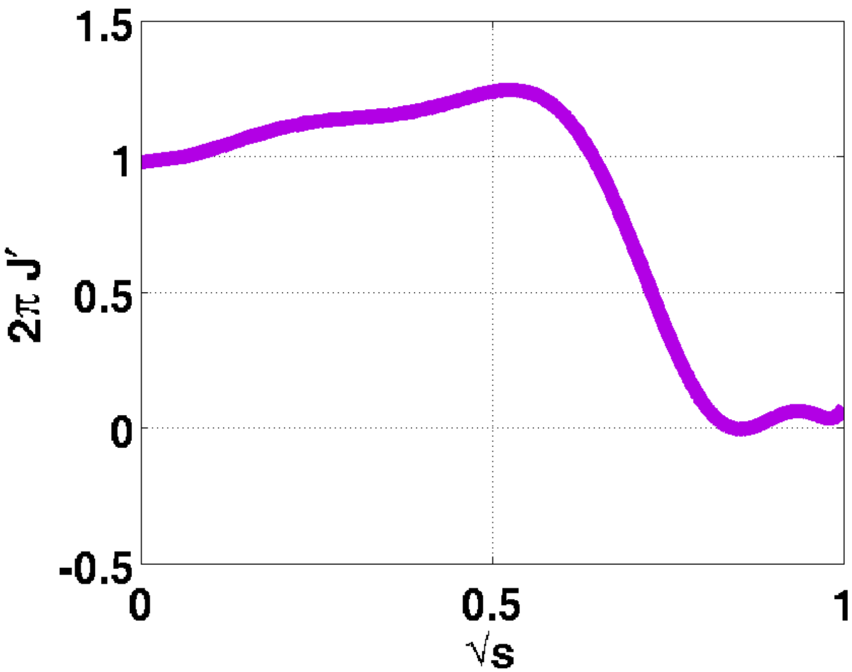

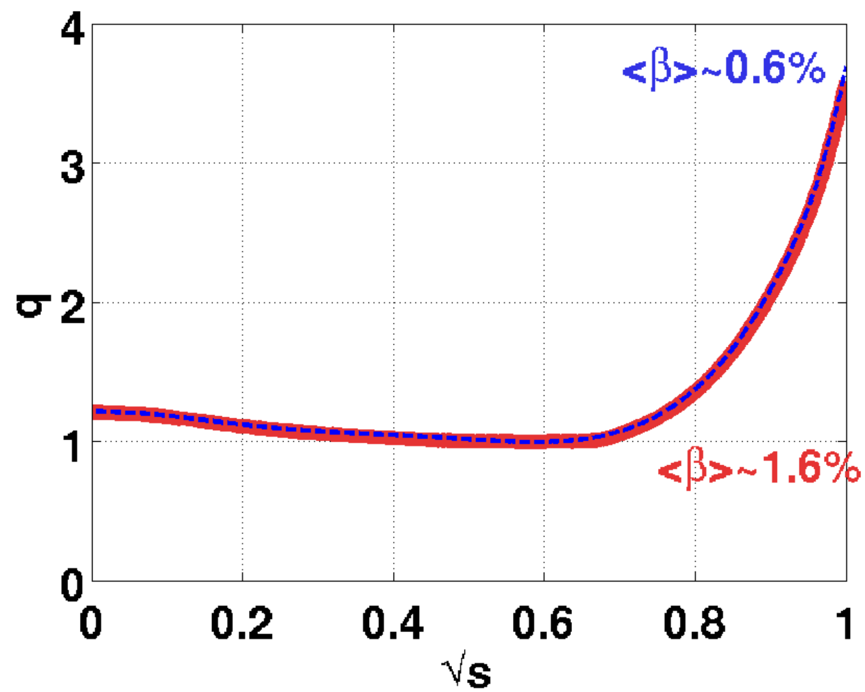

TCV pressure contour cross sections at different $\langle\beta\rangle$

- $\langle\beta\rangle \sim 0.6\%,\ 2\pi J = 493kA,\ q_{min} = 0.995$

$v = 0$ $\quad v = \pi/3$ $\quad v = 2\pi/3$ $\quad v = \pi$

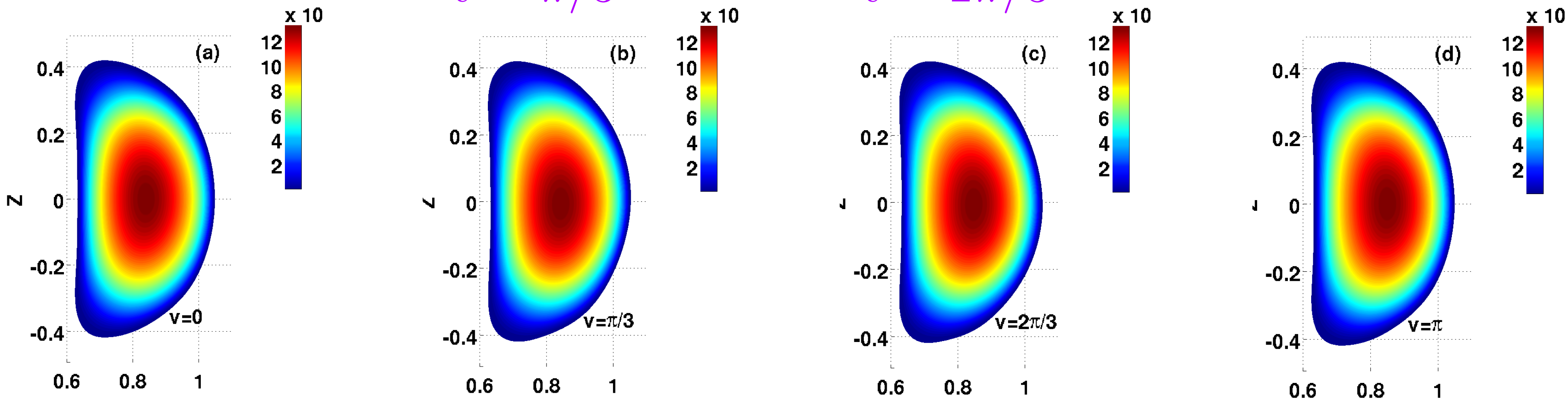

- $\langle\beta\rangle \sim 1.6\%,\ 2\pi J = 485kA,\ q_{min} = 0.995$ —- helical branch

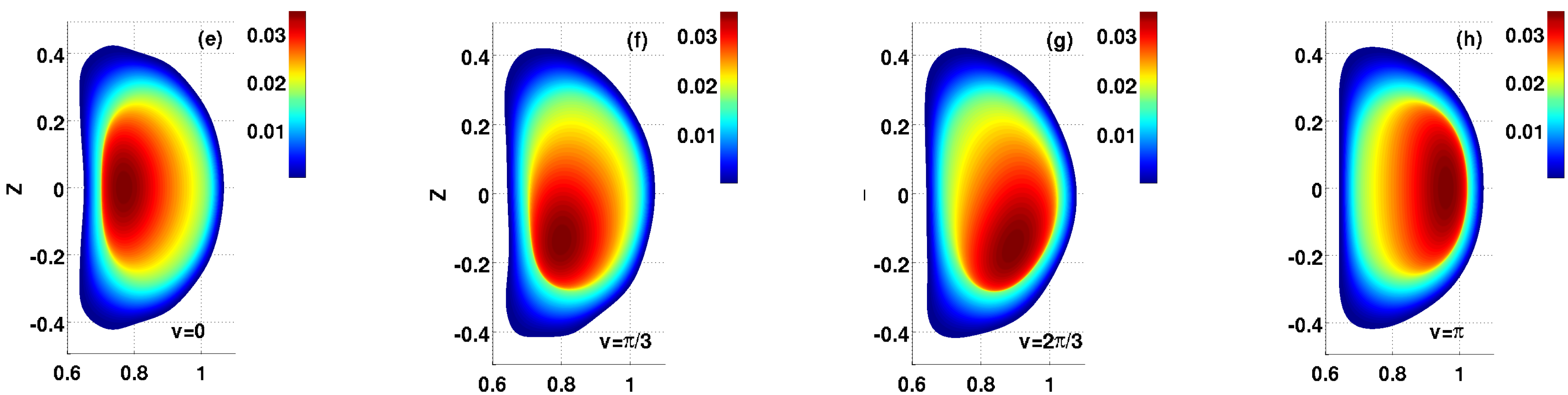

R $\quad R$ $\quad R$ $\quad R$

TCV Axis Excursion with $\langle\beta\rangle$ and q_{min}

- Pressure profile prescribed as $p(s) = p(0)(1-s)(1-s^4)$
- Variation of δ_H with $\langle\beta\rangle$ at $q_{min} = 0.995$ with q_{min} at $\langle\beta\rangle = 1.6\%$

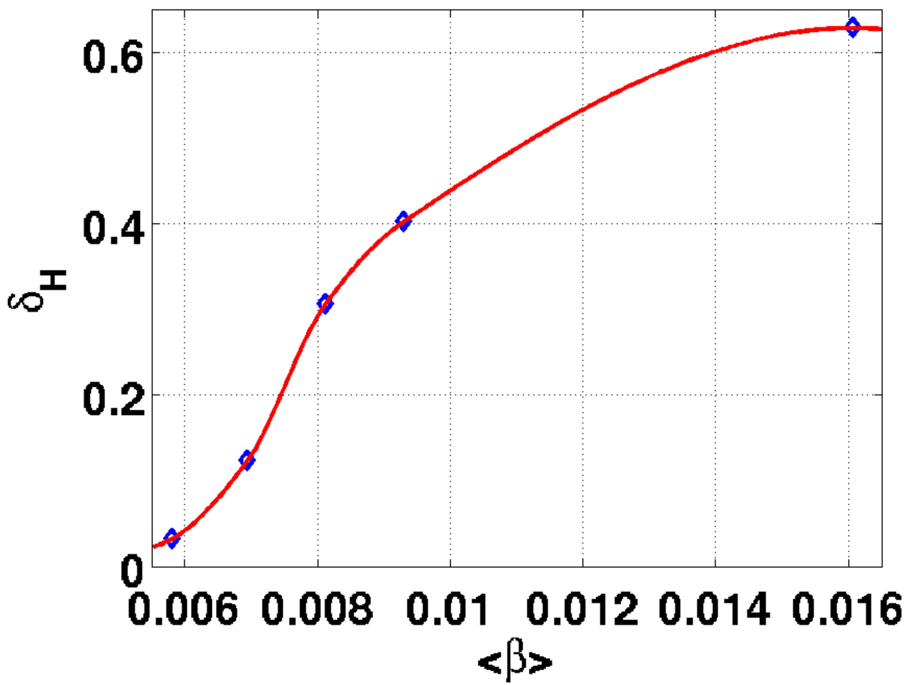

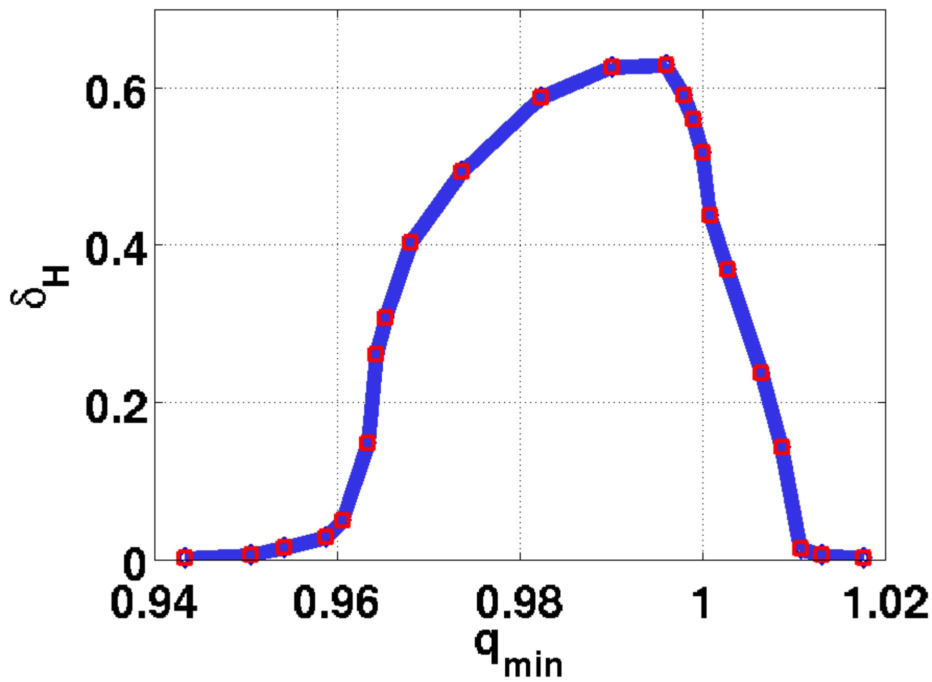

- Helical core develops when $\langle\beta\rangle > 0.6\%$
- Large helical core for $0.96 < q_{min} < 1.01$

TCV "snake-like" structures

- Variation of the snake size as a function of $\langle\beta\rangle$, β_N

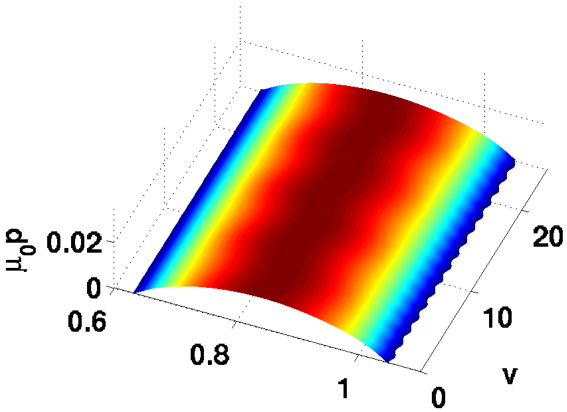

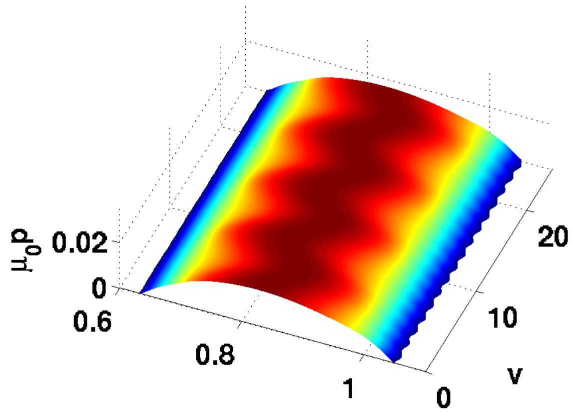

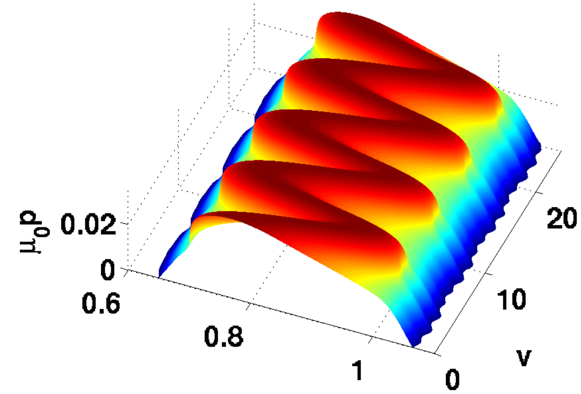

- $\langle\beta\rangle = 0.58\%$ $\quad$ $\langle\beta\rangle = 0.69\%$ $\quad$ $\langle\beta\rangle = 1.6\%$
- $\beta_N = 0.34$ $\quad$ $\beta_N = 0.41$ $\quad$ $\beta_N = 0.98$

- Snake size increases with $\langle\beta\rangle$
- Though the 3D core deformation only weakly alters the plasma-vacuum interface, there are wiggles that result from interactions of $n = 1$, $n = 2$ and $n = 3$ components.

TCV equilibria in Boozer coordinate frame

- Toroidal flux contours in Boozer coordinates

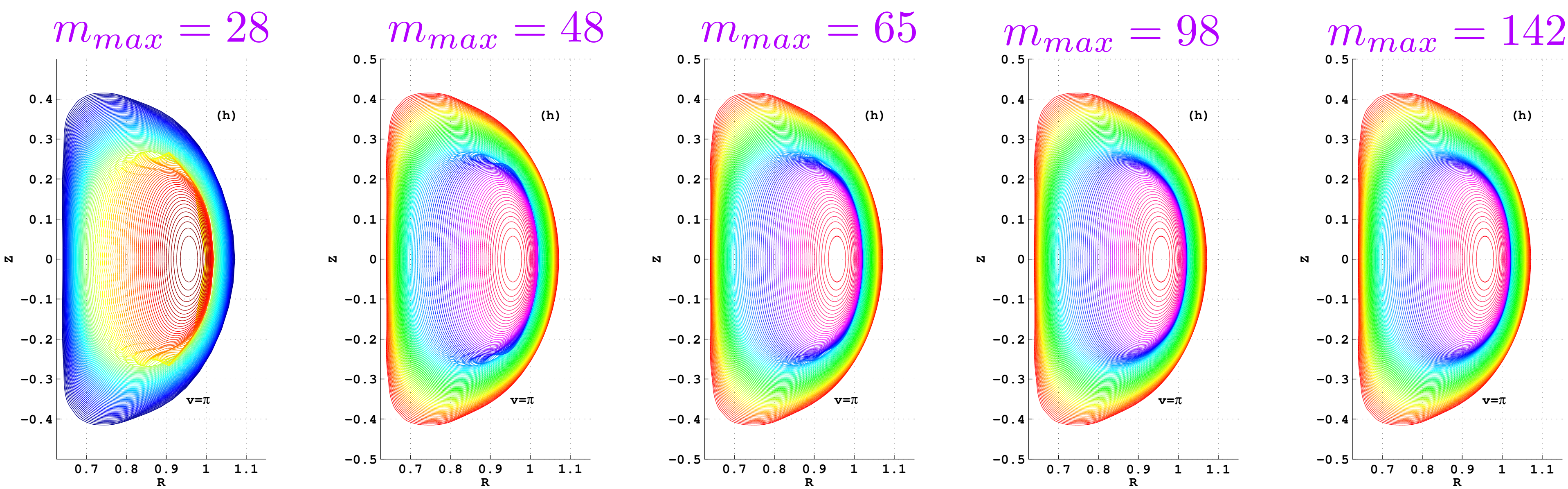

- High order resonant Boozer components must be retained for convergence

- Memory intensive computations with large number of modes

TCV Boozer mesh grid

- Boozer coordinate mesh grid shows distortions at the interface of the helical core and the axisymmetric mantle

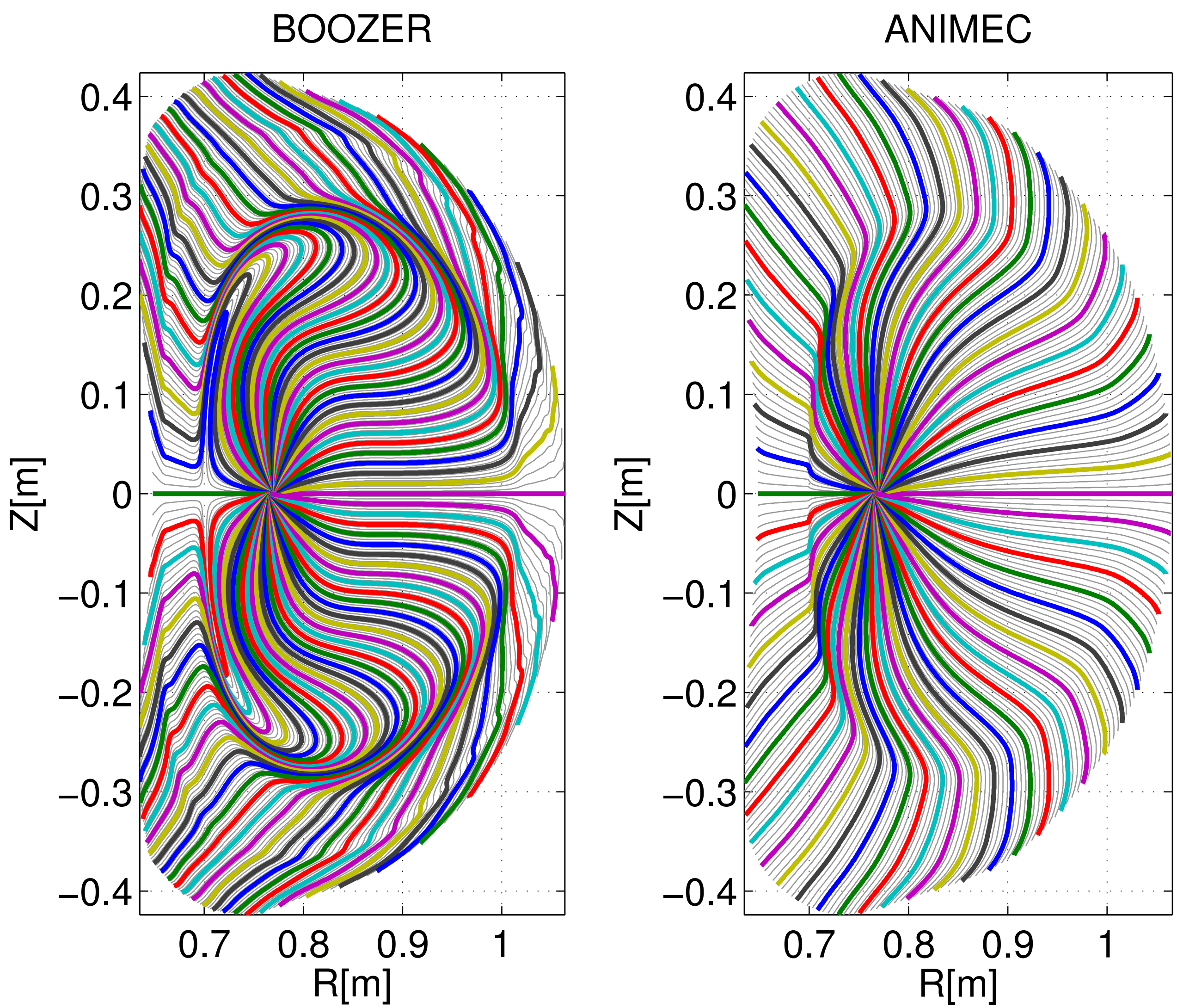

Experimental Issues and Considerations

- Contend that JET, Tore Supra, etc "snakes", TCV continuous modes, MAST long-lived modes, NSTX saturated internal kinks essentially represent the same physical phenomenon.

- Comparison with MAST Long-Lived Modes envisioned

- Experimental tests in TCV and DIII-D (a Torkil Jensen Award experiment) are planned
  Off-axis heat/CD with/without ramp-up: $q(s)$;$\langle\beta\rangle$)
  Modulated current ramp-up/ramp-down: (q_{min})
  Ar impurity injection to trigger snake: (N_e)
  New RT control and procedure to optimise actuator trajectory to quickly identify best options (*F. Felici, O. Sauter, PPCF **54** (2012) 025002*)

Summary and Conclusions ..(1)

- Nominally axisymmetric Tokamak systems can develop MHD equilibrium bifurcations leading to core helical structures even when a fixed axisymmetric boundary is imposed.
- In Tokamak devices, reversed magnetic shear (or extended low shear) with $q_{min} \sim 1$ can trigger bifurcated solutions with a core helical structure similar to a saturated ideal $1/1$ internal kink.
- Fixed boundary simulations in JET, ITER and DIII-D and free boundary calculations that model TCV show that equilibria with large internal 'snake-like' $1/1$ helical structures can be obtained.
- Model predicts 'snake' structures in the range $0.94 < q_{min} < 1.03$ in JET. A $q = 1$ island is not required for 'snake' formation and persistence.
- The plasma-vacuum interface is not strongly deformed by the internal helical structure, though wiggles due to $n = 1, 2, 3$ interactions appear at the outer edge.

Summary and Conclusions ..(2)

- The 3D helical core equilibrium states in nominally axiymmetric systems that have been obtained constitute a paradigm shift which compels the application of tools developed for stellarators in MHD stability, kinetic stability, drift orbits, wave propagation or heating, neoclassical transport, gyrokinetics, etc to tokamak magnetic confinement physics research.

- The Boozer magnetic coordinate spectrum must be broadened extensively to faithfully reproduce the interface between the helical core and the axisymmetric mantle.

- The constraint of nested magnetic flux surfaces and absence of X-points in our model preclude the generation of equilibrium states with magnetic islands. Saturated tearing modes could be investigated with SIESTA, PIES, HINT and SPEC equilibrium codes or with nonlinear MHD codes like XTOR and M3D.

Publications

- *Tokamak Magnetohydrodynamic Equilibrium States with Axisymmetric Boundary and a 3D Helical Core*
  W. A. Cooper, J. P. Graves, A. Pochelon, O. Sauter and L. Villard, Phys. Rev. Lett. **105** (2010) 035003.

- *Helical ITER Hybrid Scenario Equilibria*
  W. A. Cooper, J. P. Graves and O. Sauter, Plasma. Phys. Control. Fusion **53** (2011) 024002.

- *Magnetohydrodynamic Properties of Nominally Axisymmetric Systems with 3D Helical Core*
  W. A. Cooper, J. P. Graves, O. Sauter, I. T. Chapman, M. Gobbin, L. Marrelli, P. Martin, I. Predebon and D. Terranova, Plasma. Phys. Control. Fusion **53** (2011) 074008.
  2010 ICPP special issue.

Publications

- *MHD Equilibrium and Stability of Tokamak and RFP Systems with 3D Helical Cores*
  W. A. Cooper, J. P. Graves, O. Sauter, D. Terranova, M. Gobbin, L. Marrelli, P. Martin and I. Predebon, Plasma. Phys. Control. Fusion **53** (2011) 084001.
  2010 MHD Workshop special issue.

- *JET Snake Magnetohydrodynamic Equilibria*
  W. A. Cooper, J. P. Graves and O. Sauter, Nucl. Fusion **51** (2011) 072002.

- *Helical Core Tokamak MHD Equilibrium States*
  W. A. Cooper, J. P. Graves, O. Sauter, J. Rossel, M. Albergante, S. Coda, B. P. Duval, B. Labit, A. Pochelon, H. Reimerdes and the TCV team, Plasma. Phys. Control. Fusion **53** (2011) 124005.
  2011 EPS special issue.

THEORY REVIEW

- Analytic investigations of nonlinearly saturated $m = 1, n = 1$ ideal MHD instability
  - Avinash, R.J. Hastie, J.B. Taylor, Phys. Rev. Lett. **59** (1987) 2647
  - M.N. Bussac, R. Pellat, Phys. Rev. Lett. **59** (1987) 2650
  - F.L. Waelbroeck, Phys. Fluids **B 1** (1989) 499
- Large scale simulations of nonlinearly saturated MHD instability
  - L.A. Charlton et al., Phys. Fluids **B 59** (1989) 798
  - H. Lütjens, J.F. Luciani, J. Comput. Phys. **227** (2008) 6944
- Bifurcated equilibria due to ballooning modes with the NSTAB code
  - P. Garabedian, Proc. Natl. Acad. Sci. USA **103** (2006) 19232
- RFX-mod SHAx MHD equilibria
  - D. Terranova et al., PPCF **52** (2010) 124023
- Bifurcated tokamak equilibria similar to a saturated internal kink
  - W.A. Cooper et al., Phys. Rev. Lett. **105** (2010) 035003

Fixed Boundary Bean-shaped DIII-D Computation

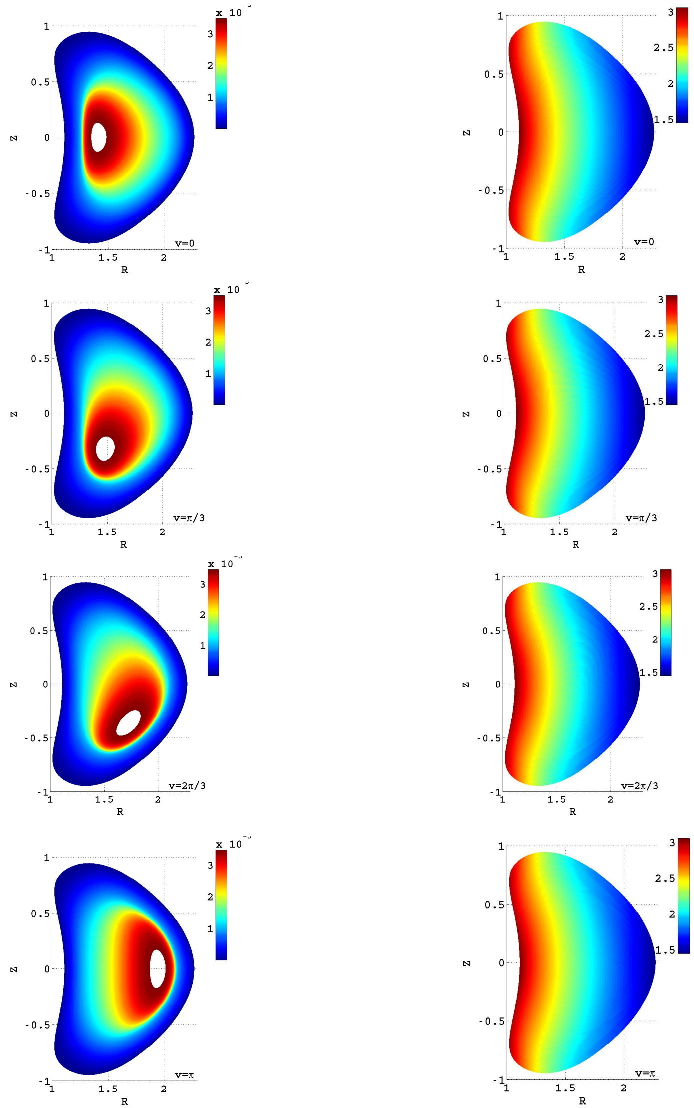

Fig. 1. The normalised plasma pressure (left column) and the mod-B (right column) distributions in a fixed axi- and up-down symmetric boundary hybrid-scenario DIII-D equilibrium calculation at 4 cross sections covering half a field period with toroidal angles $v = 0$, $v = \pi/3$, $v = 2\pi/3$ and $v = \pi$ (top to bottom row, respectively) at $\langle\beta\rangle \simeq 0.55\%$ and $2.3MA$ toroidal current.

1

Bifurcated equilibria in TCV

- Selection of q-profiles that yield bifurcated equilibria in TCV.
- Boundary description: $R_b = 0.8 + 0.2\cos u + 0.06\cos 2u, \quad Z_b = 0.48\sin u.$
- $q = (0.5+s-1.1s^4)^{-1}$, $(0.7+0.7s-s^4)^{-1}$, $(0.9+0.2s-0.8s^6)^{-1}$, $(0.98-0.7s^9)^{-1}$.

Convergence of solutions

- Define helical excursion parameter

$$\delta_H = \frac{\sqrt{R_{01}^2(s=0) + Z_{01}^2(s=0)}}{a}$$

- Convergence of δ_H with N_r = number of radial grid points

TCV pressure contour cross sections at different $\langle\beta\rangle$

- $\langle\beta\rangle = 0.55\%$ —- axisymmetric branch

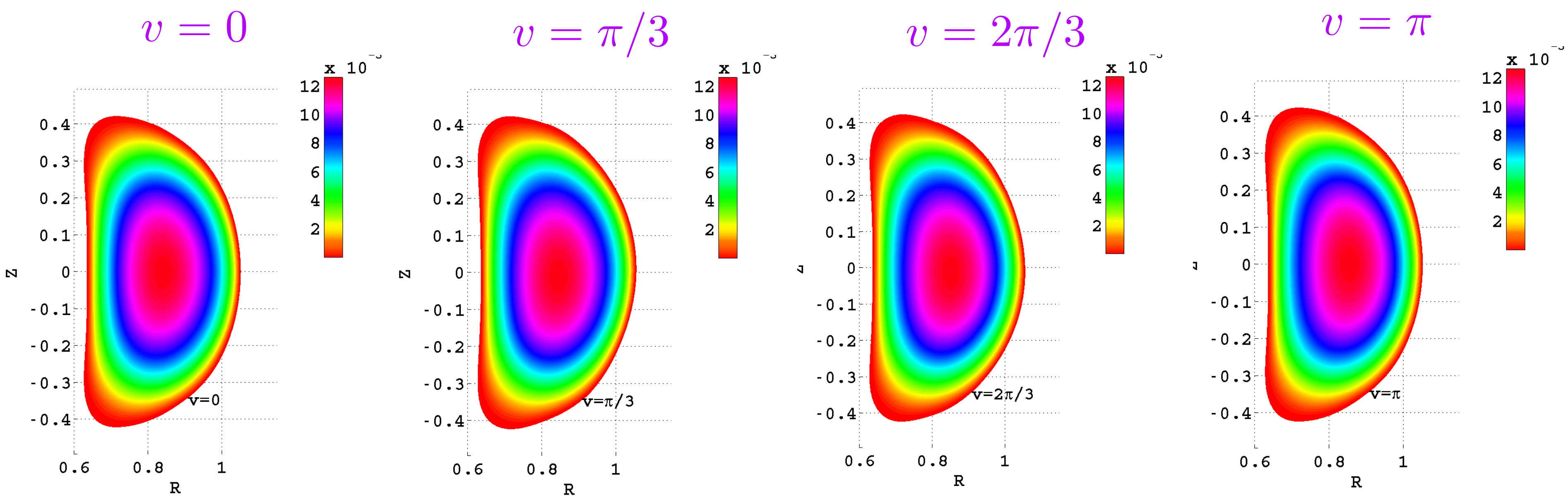

- $\langle\beta\rangle = 1.1\%$ —- helical branch

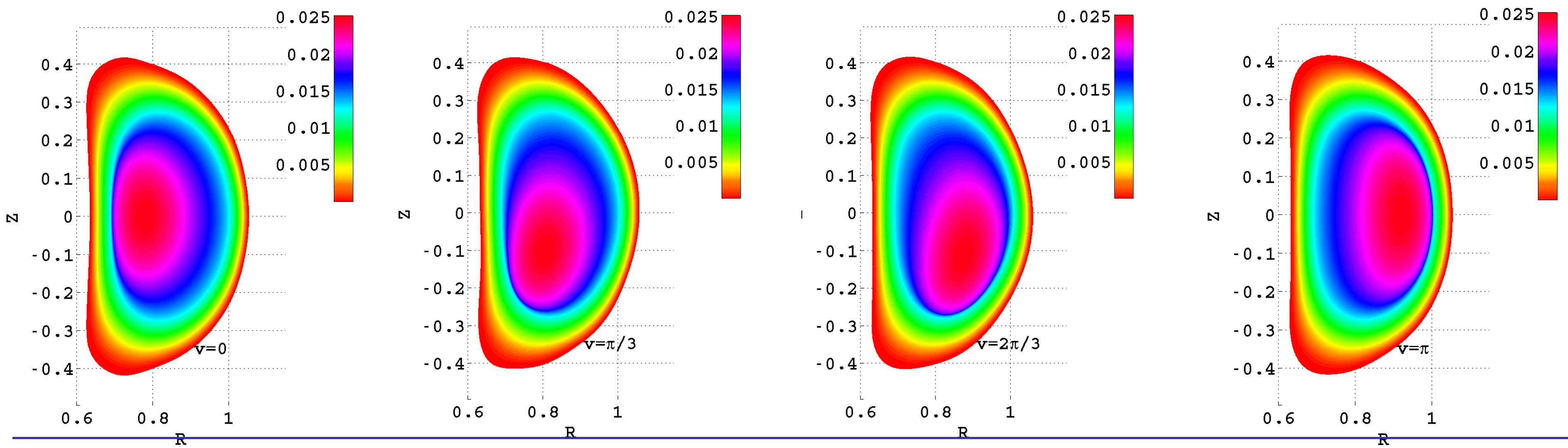

TCV free boundary equilibrium convergence

- Convergence to a solution and average radial force balance

- horizontal force normalised radial force

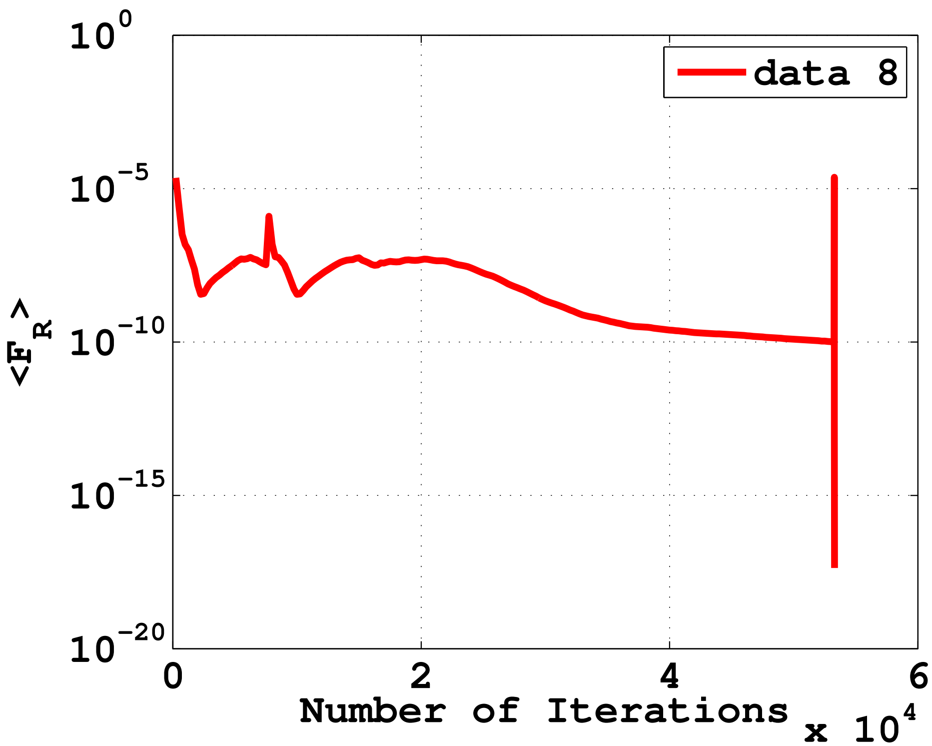

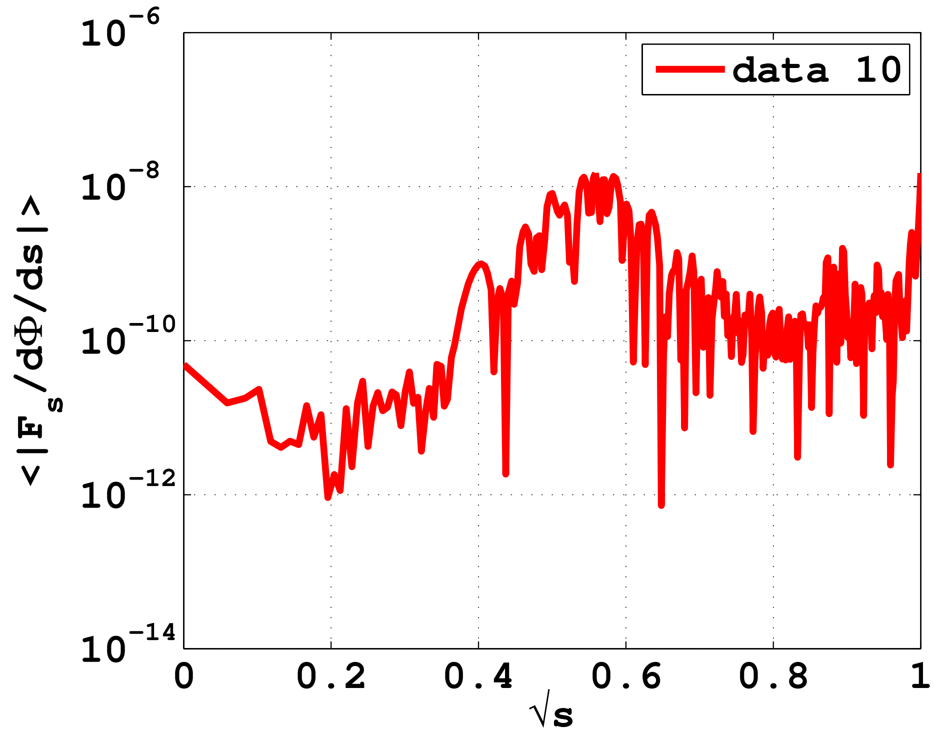

TCV Boundary

- For $q(s) = [0.9 + 0.43s - 0.1s^3 - 4.535s^4 + 3.405s^5]^{-1}$ and $\langle\beta\rangle = 1.7\%$.

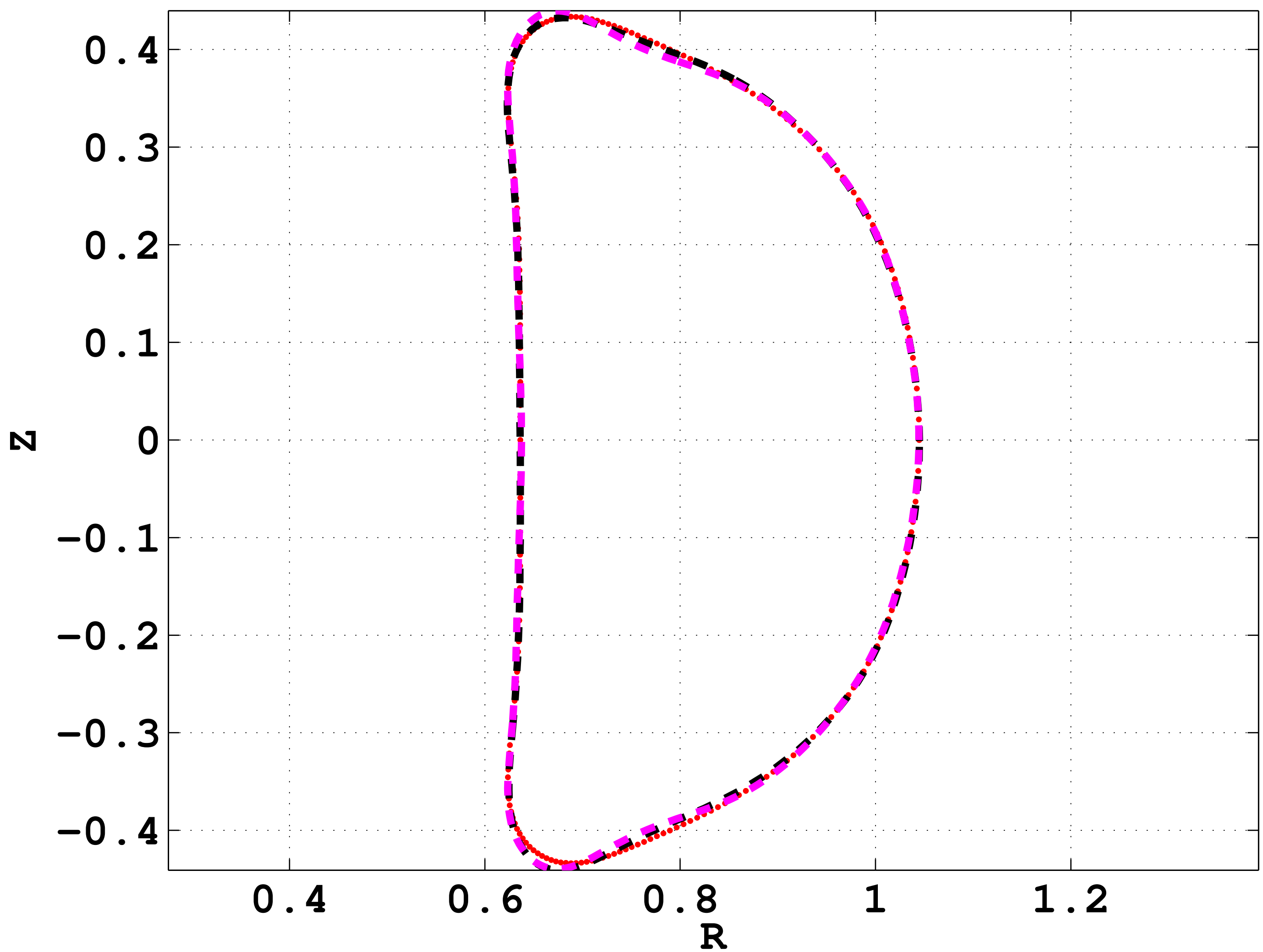

Boundaries for TCV, ITER, MAST and JET

- Fixed axisymmetric boundary equilibrium studies are explored.
- TCV boundary description: $R_b = 0.8 + 0.2\cos u + 0.06\cos 2u; \quad Z_b = 0.48\sin u$
- MAST, JET boundary: $R_b = R_0 + a\cos(u + \delta\sin u + \tau\sin 2u); \quad Z_b = Ea\sin u$
  MAST: $R_0 = 0.9m$, $a = 0.54m$, $E = 1.744$, $\delta = 0.3985$, $\tau = 0.1908$
  JET: $R_0 = 2.96m$, $a = 1.25m$, $E = 1.68$, $\delta = 0.3$, $\tau = 0$

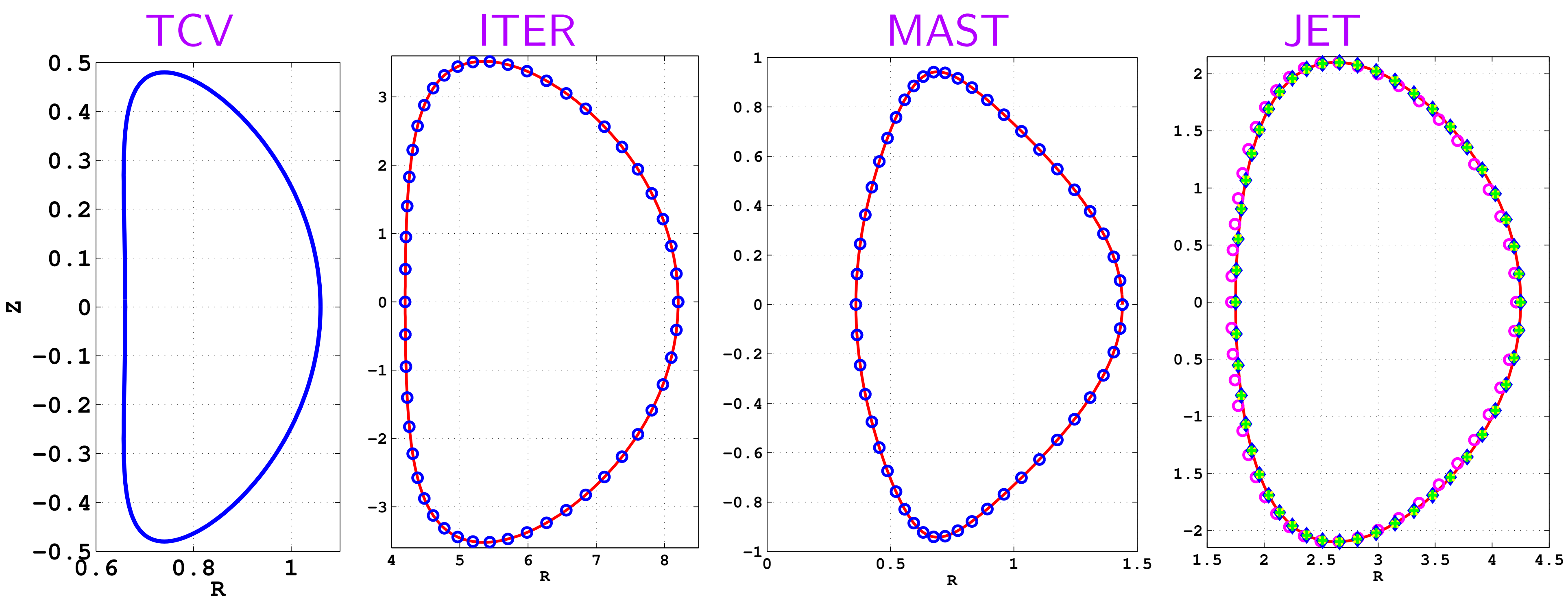

Fixed boundary MAST computation

- Contours of constant pressure of a MAST equilibrium
- W. A. Cooper, J. P. Graves, O. Sauter, I. T. Chapman, M. Gobbin, L. Marrelli, P. Martin, I. Predebon and D. Terranova, Plasma. Phys. Control. Fusion **53** (2011) 074008.

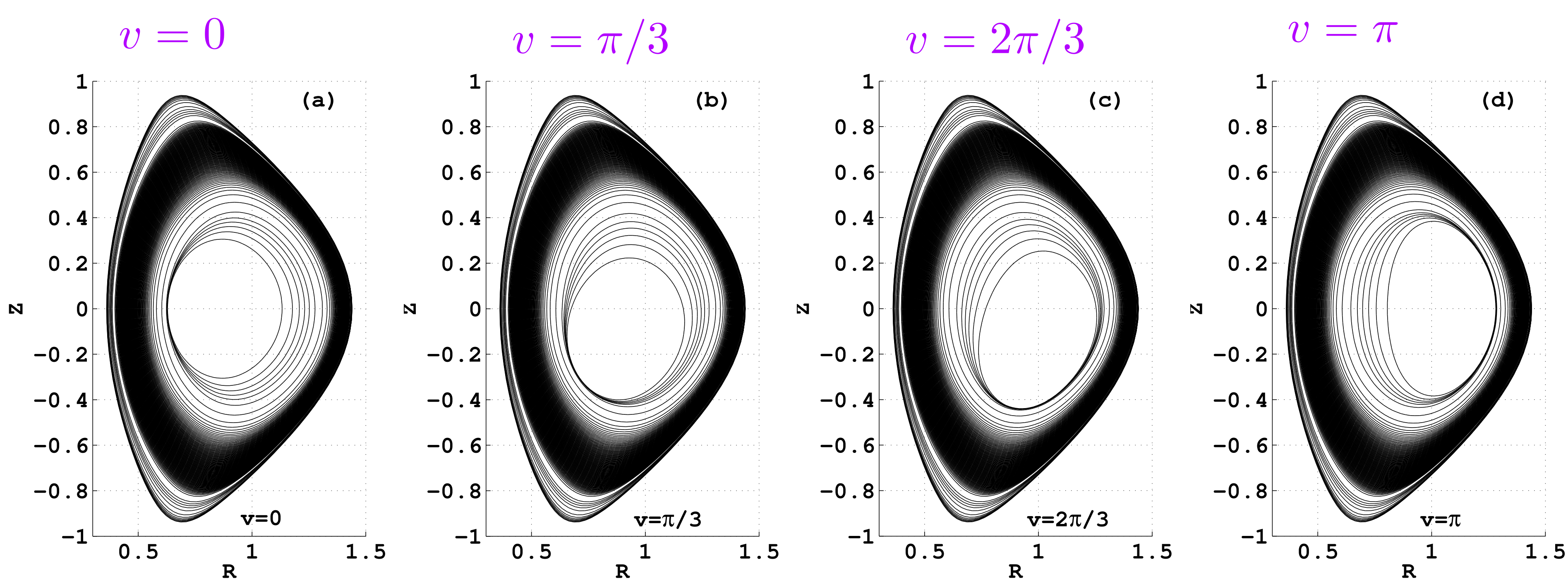

Free Boundary MAST Computations

- MAST coil system — 4 filaments per coil

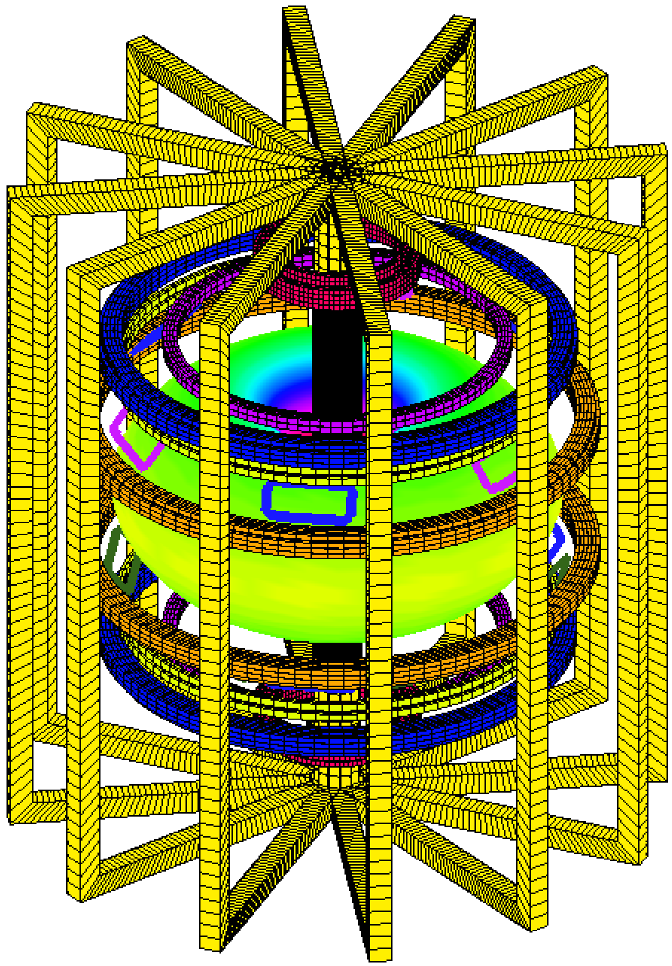

MAST profiles

- $p(s) = p(0)(1-s)(1-s^4)$; $2\pi J'(s) = 2\pi J'(0)[1.7(1-s^2)^2 - 0.7(1-s)^2]$

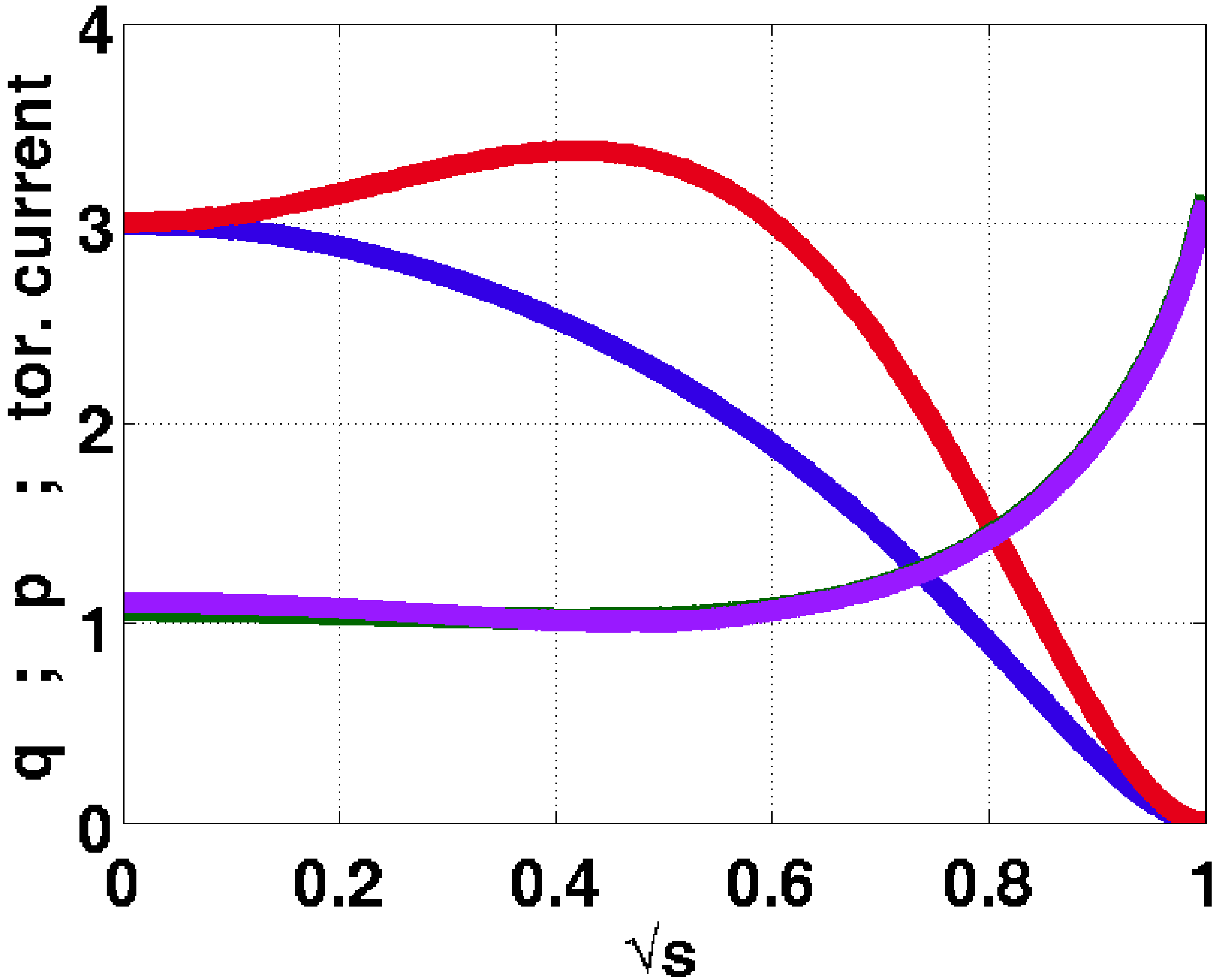

MAST pressure contour cross sections

- $\langle\beta\rangle \sim 6\%$, $2\pi J = 842kA$ —- axisymmetric branch

$v = 0$ $\quad v = \pi/3$ $\quad v = 2\pi/3$ $\quad v = \pi$

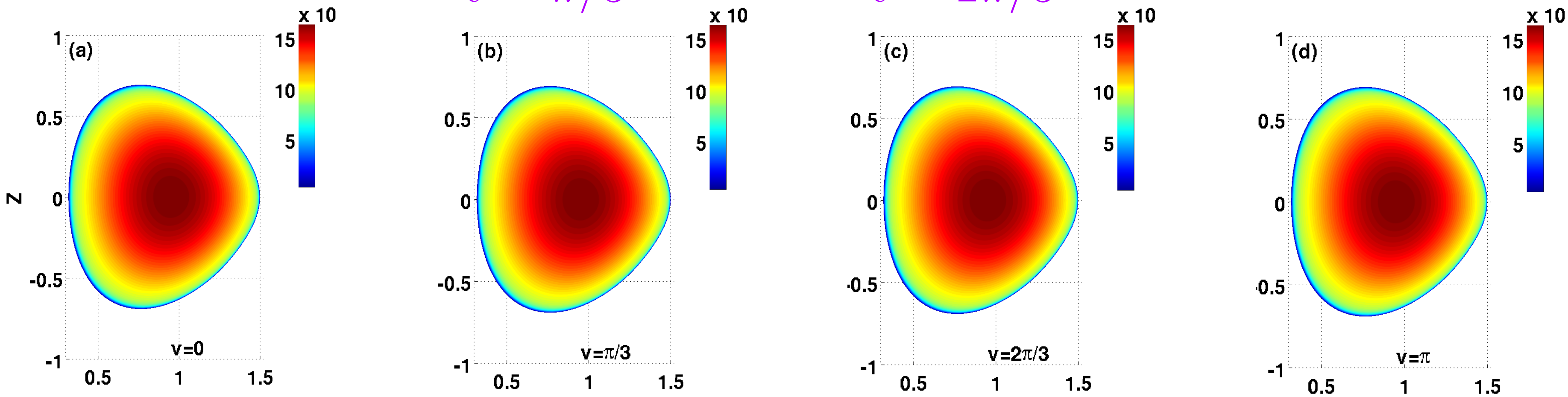

- $\langle\beta\rangle \sim 6\%$, $2\pi J = 842kA$ —- helical branch

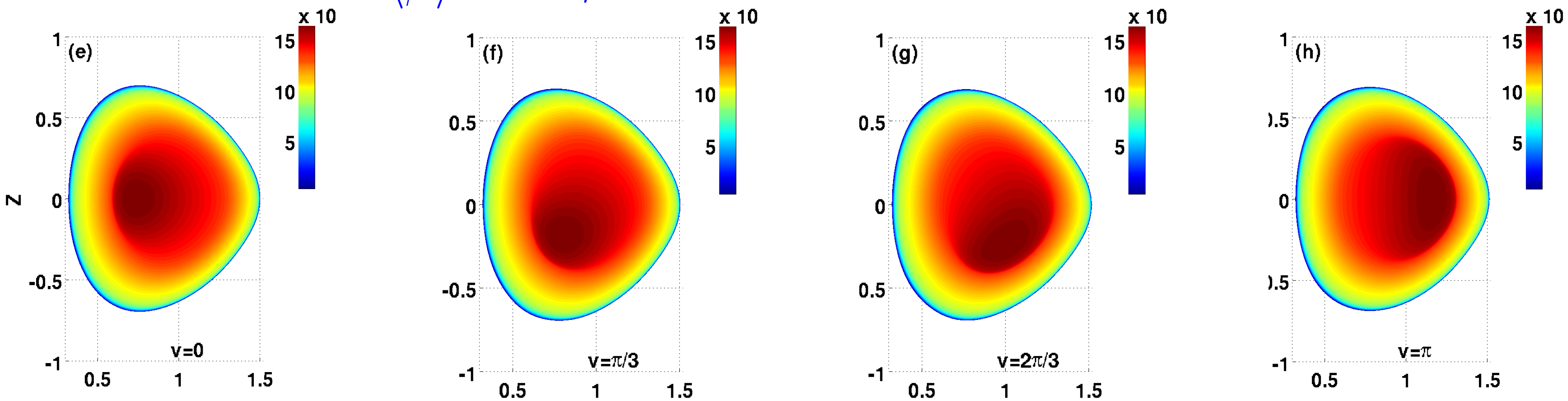

R $\quad R$ $\quad R$ $\quad R$

MAST pressure distribution at the midplane

- Axisymmetric Branch Helical Branch

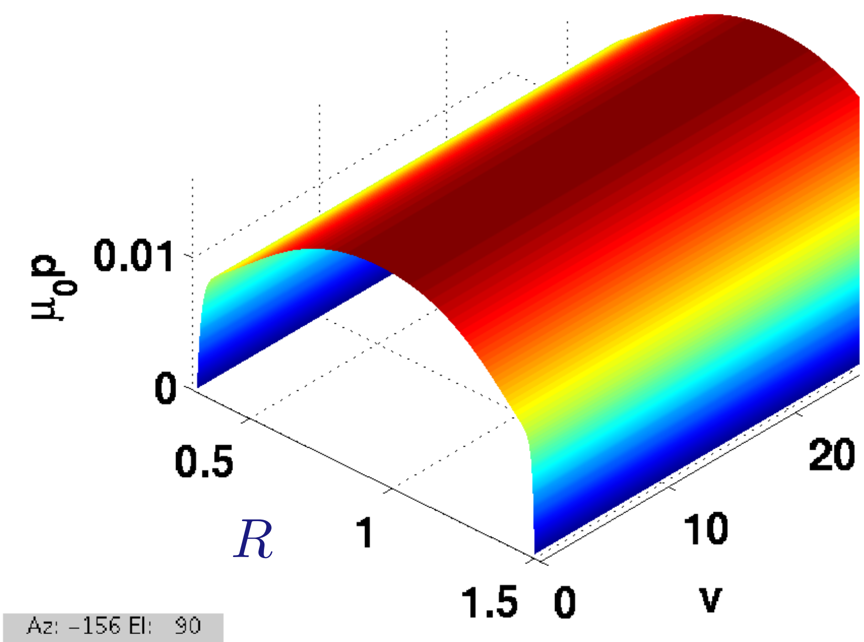

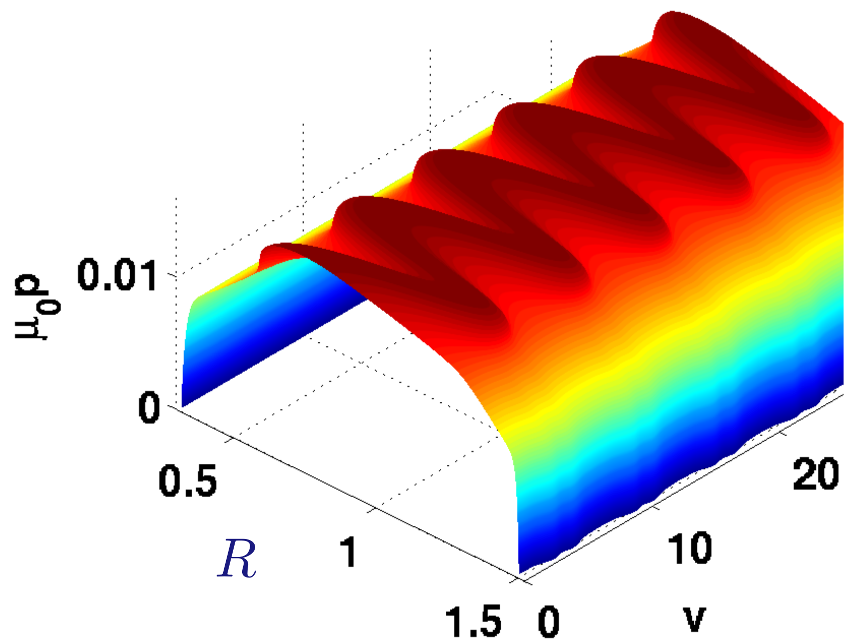

Edge R toroidal modulation

- Variation of the midplane plasma outer boundary position. The mode selection pattern ($m = 0 \rightarrow 11$,$n = -6 \rightarrow +6$) suppresses the ripple effect ($n = 12$)

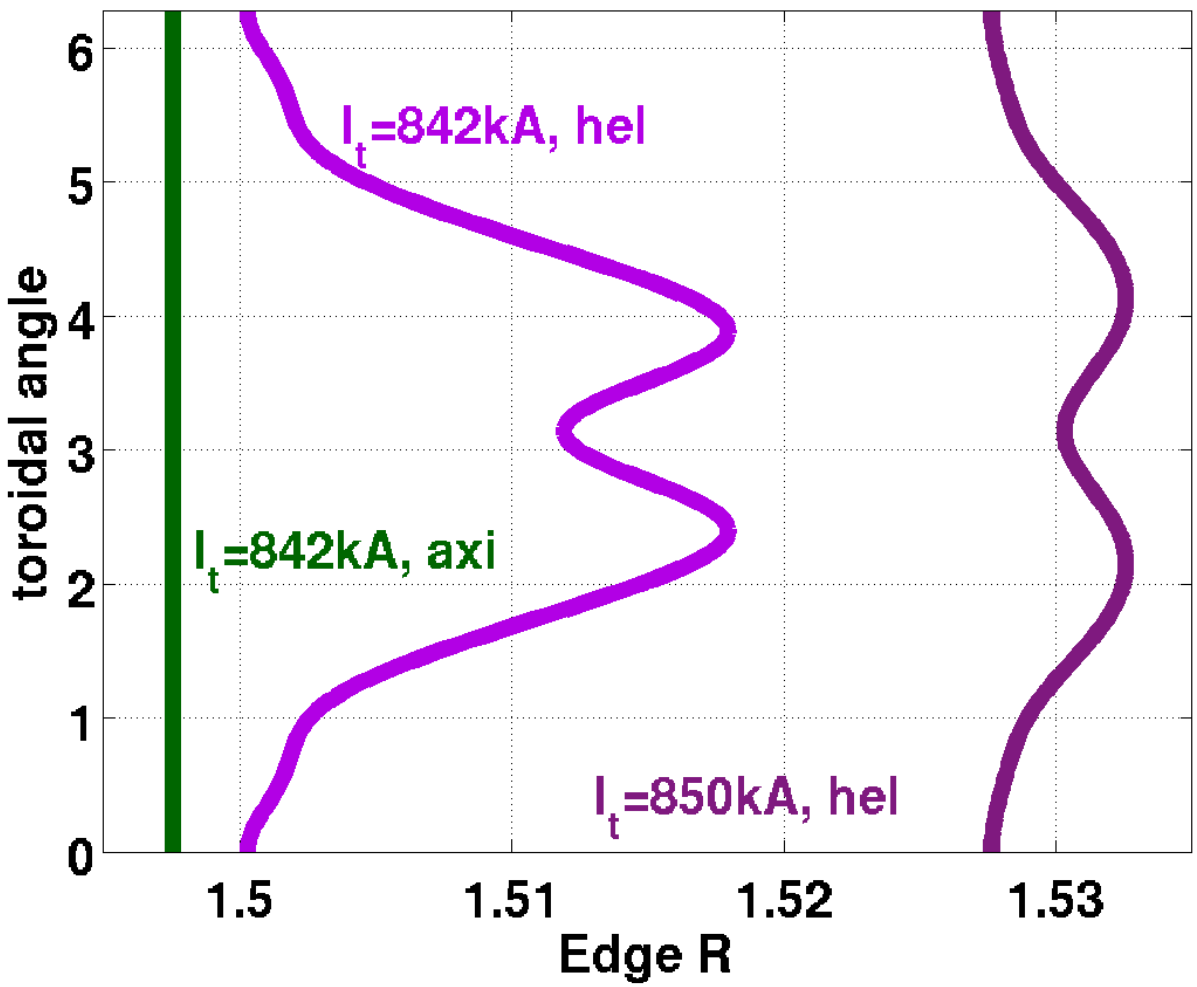

TCV Coil Data

- All coils are described by 4 filaments, one at each vertex, to yield the correct coil dimensions
- The toroidal coils carry a total current of $358kA$
- This yields $B_t = 1.3T$ at $R = 0.88m$
- There are 16 poloidal field coils that typically allow up to $238kA$

COIL LABEL	Current (kA)	number of turns	Total Current (kA)
TF	59.6226667	6	357.736
$E1;E8$	-1.7647058	34	-60
$E2;E7$	-1.1764706	34	-40
$E3;E6$	-0.2352941	34	-8
$E4;E5$	$+4.9176471$	34	$+167.2$
$F1;F8$	$+1.1111111$	36	$+40$
$F2;F7$	$+1.3333333$	36	$+48$
$F3;F6$	$+1.4444444$	36	$+52$
$F4;F5$	$+1.7777778$	36	$+64$

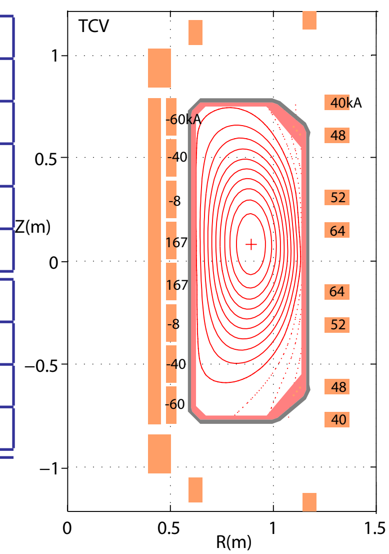

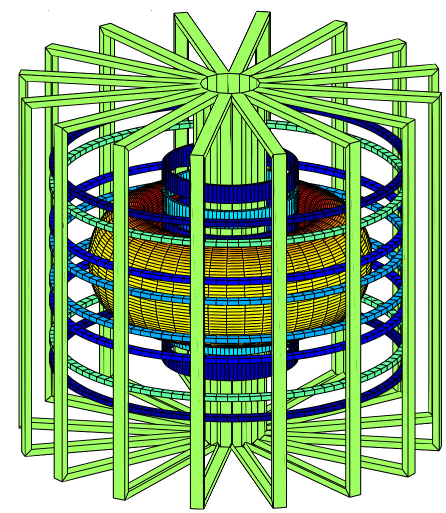

Free Boundary TCV Computations

- TCV coil system
- Toroidal coils modelled with a single filament with $358kA$
- There are 16 poloidal field coils that typically allow up to $238kA$